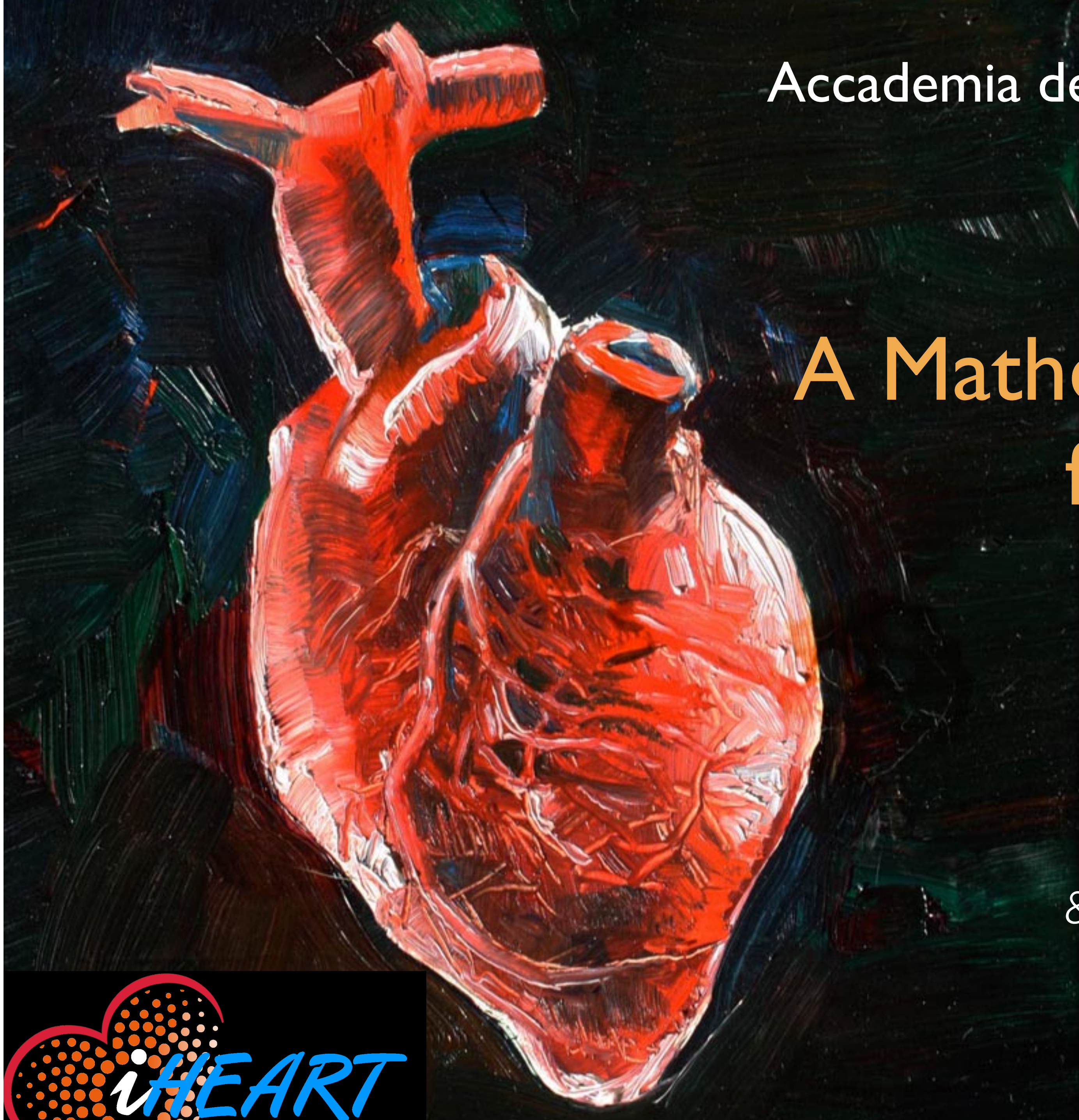

Accademia dei Lincei, 9 gennaio 2020

A Mathematical Model for the Cardiac Function

Alfio Quarteroni

MOX, Politecnico di Milano
Milan, Italy
& EPFL, Lausanne, Switzerland
(professor emeritus)

iHEART erc POLITECNICO MILANO 1863

EPFL

POLITECNICO MILANO 1863

MOX

Acknowledgments

S.Deparis, F.Menghini

(EPFL - Lausanne)

P.Zunino, C.Vergara, L.Dede', A.Manzoni,

M.Fedele, S.Pagani, I.Fumagalli, P.Africa

F.Regazzoni, S.Di Gregorio, R.Piersanti, A.Zingaro

(Politecnico di Milano**)**

R. Ruiz Baier

(U Oxford)

S. Rossi

(U North Carolina)

Local flow analysis past carotid bifurcation

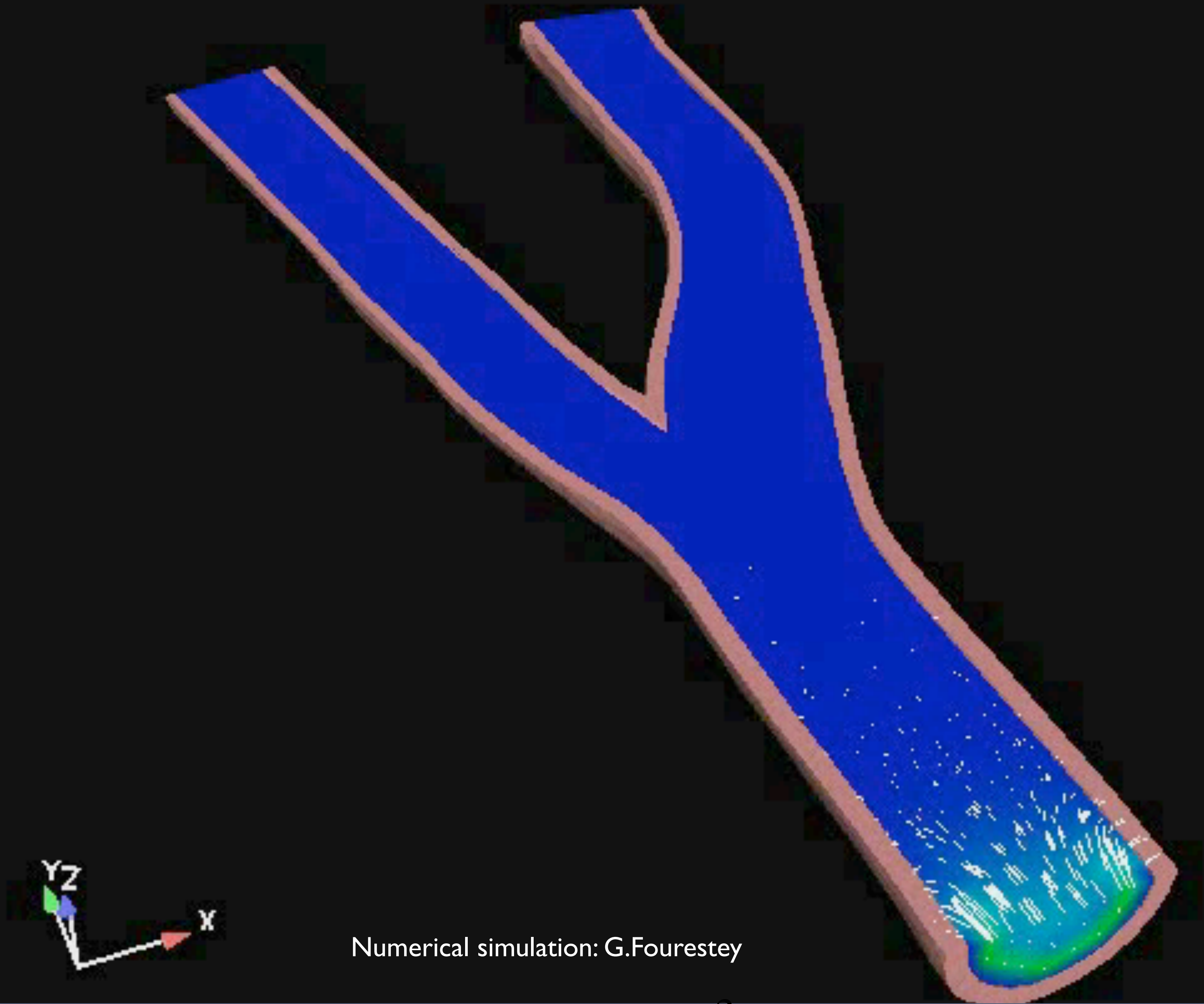

Numerical simulation: G.Fourestey

Thoracic and abdominal aorta fluid-structure simulation

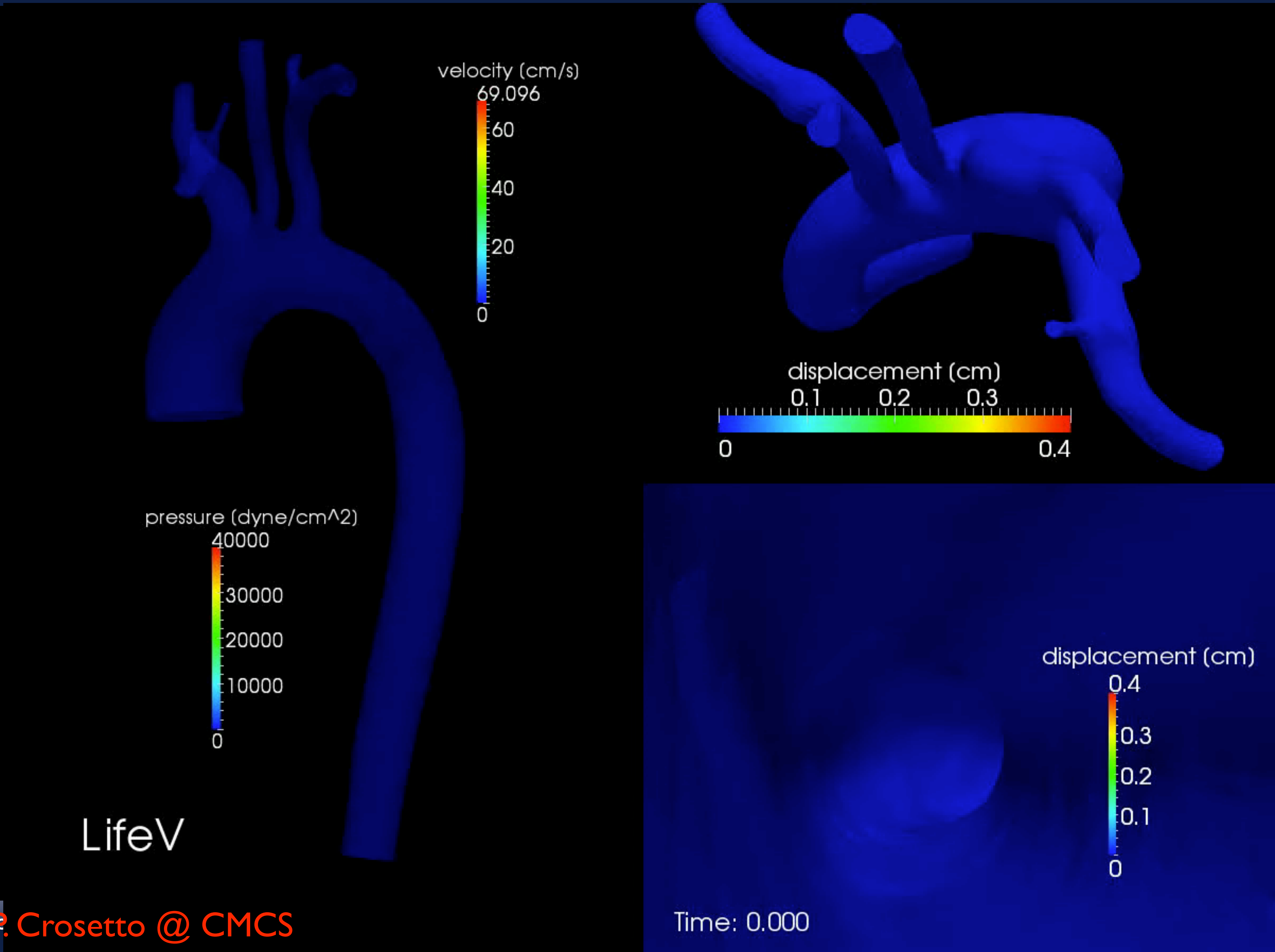

P. Crosetto @ CMCS

The Heart and the Circulation

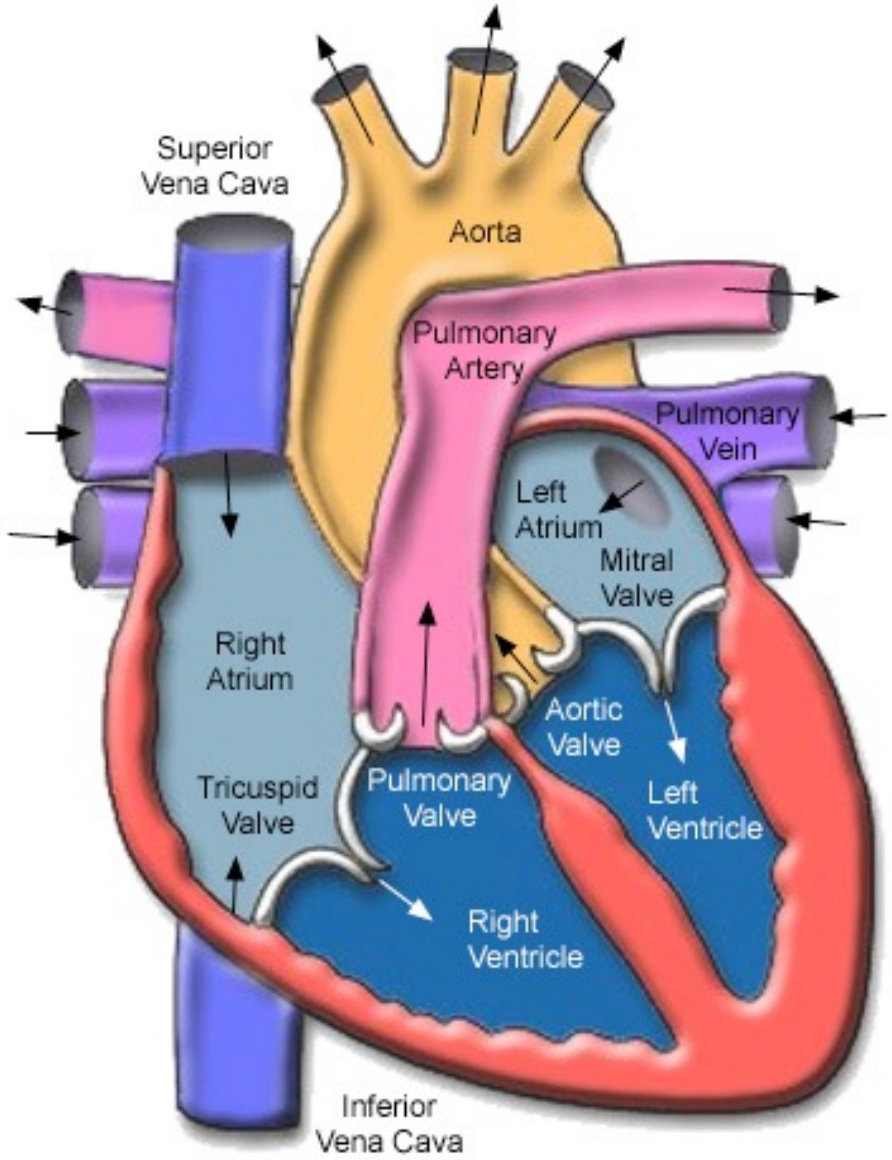

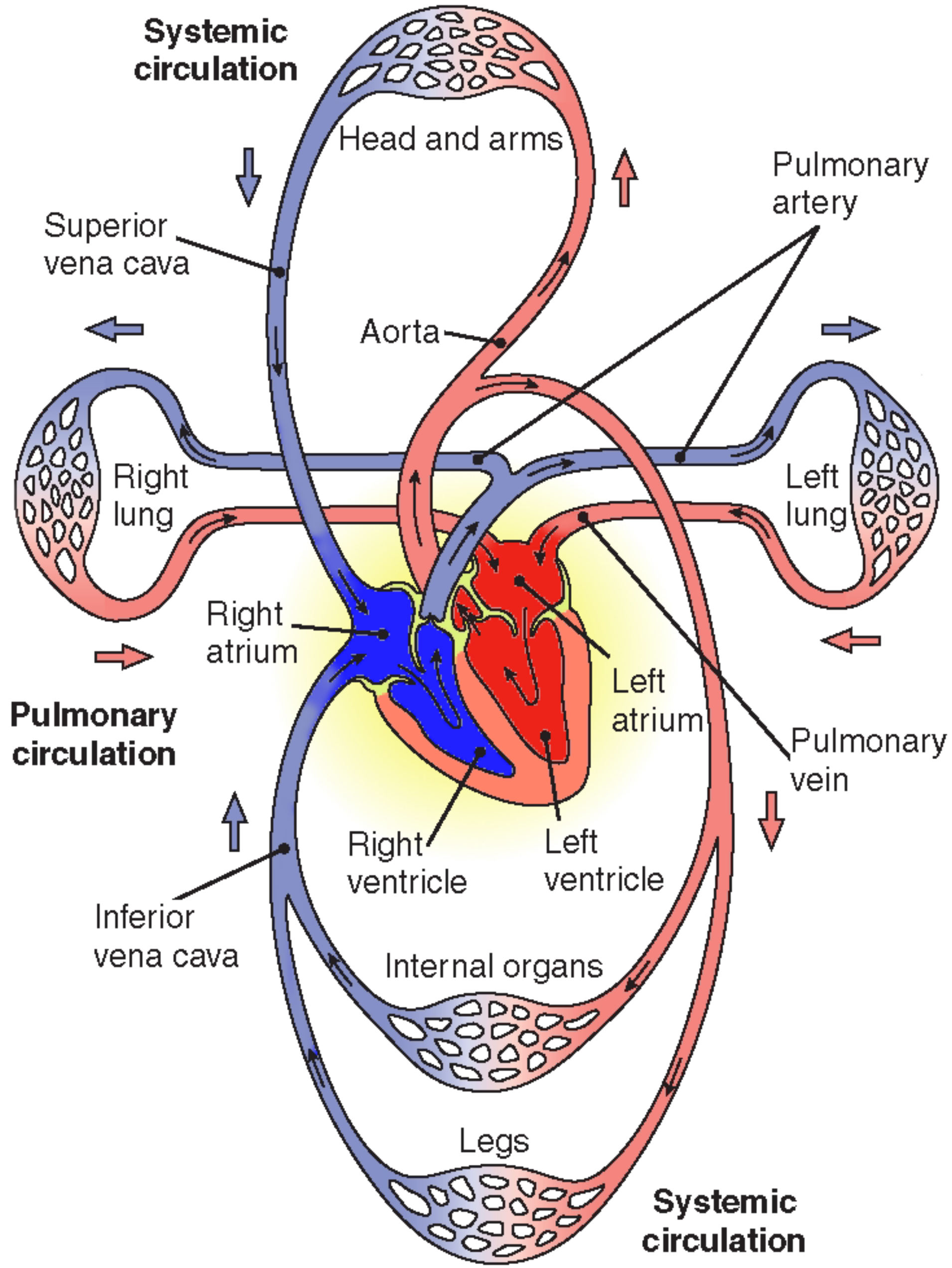

Cardiac anatomy

iHEART

erc

POLITECNICO

Cardiac Electrical Activity

Each heartbeat is triggered by an electrical signal, originating at the sinoatrial node, a natural pacemaker consisting of a cluster of self-excitable cells and located on the upper part of the RA. The electrical signal propagates from cell to cell through the two atria and it reaches the atrioventricular node, located between the atria and the ventricles.

The purpose of the atrioventricular node is acting as a filter between the atria and the ventricles in order to ensure the correct delay between the contraction of the former and the latter. This is crucial to guarantee that the ventricle contraction starts only when the blood has been pumped by the atria into the ventricles themselves.

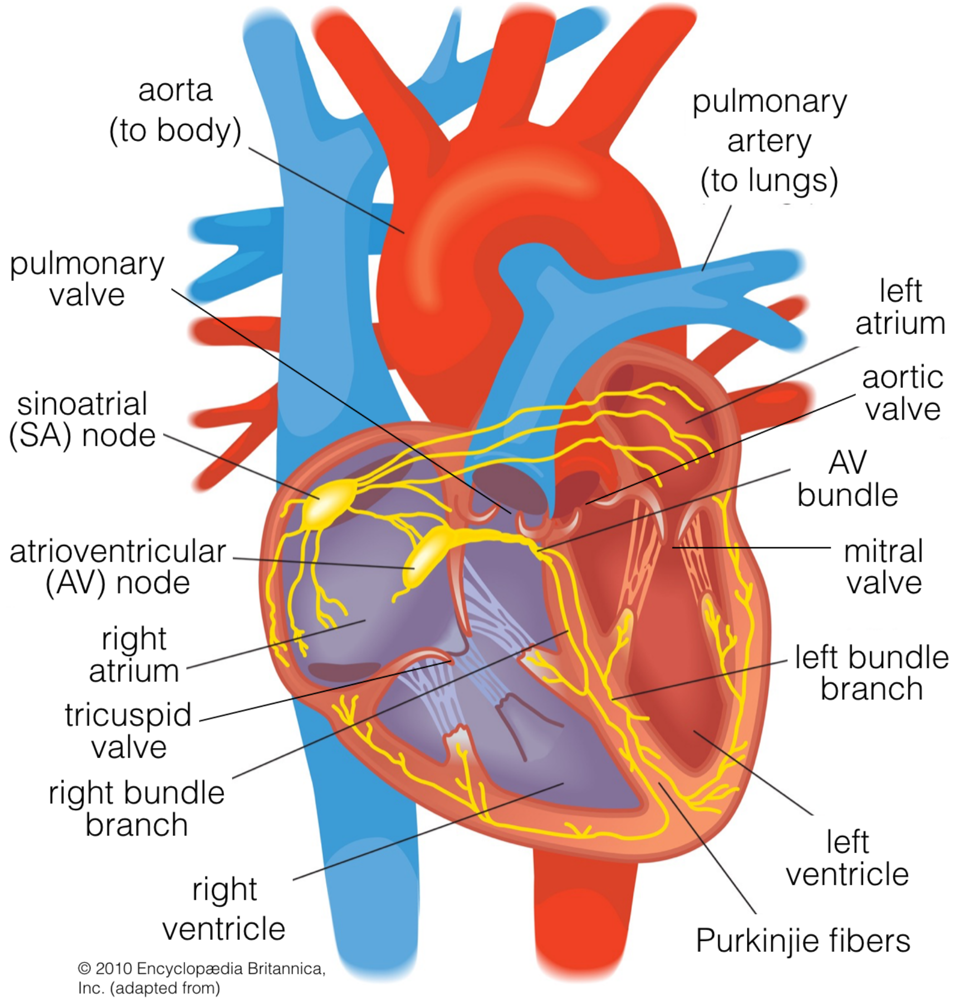

Cardiac Electrical Activity

The electrical signal travels from the atrioventricular node through a system of specialized conducting fibers, the so-called Purkinje network, and it reaches the ventricles wall. Then, similarly to what happens in the atria, it travels from cell to cell through the gap junctions.

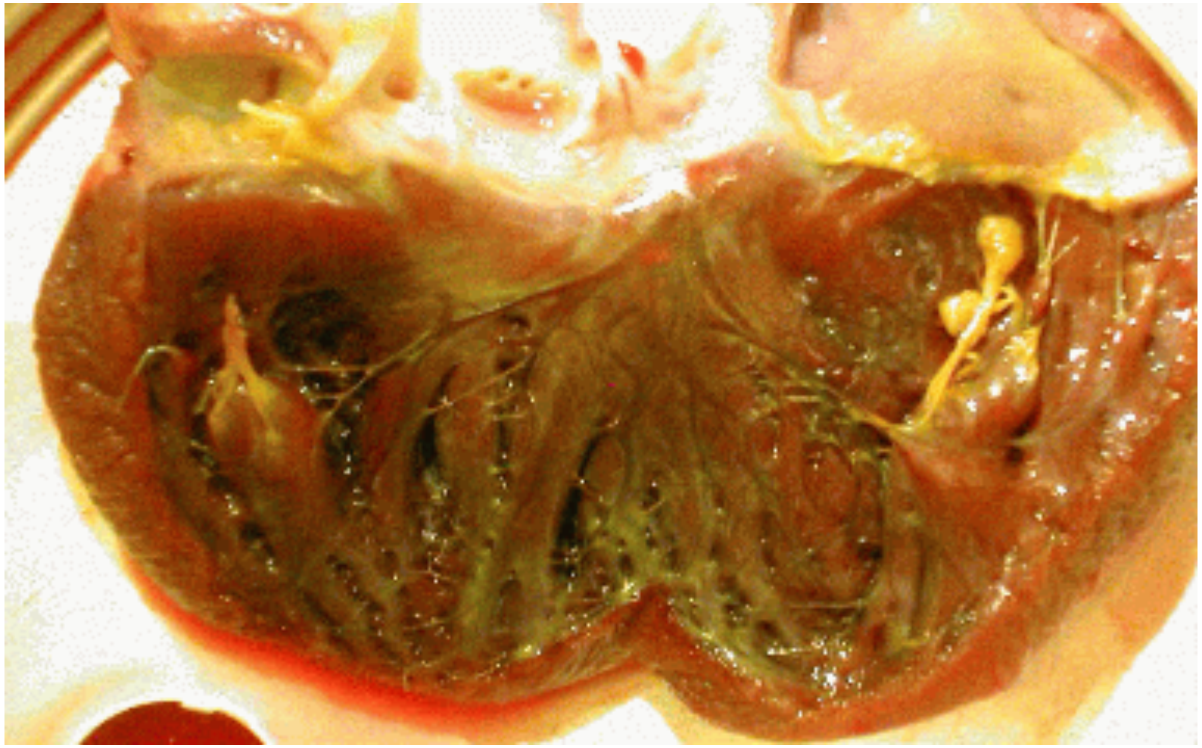

Heart apex

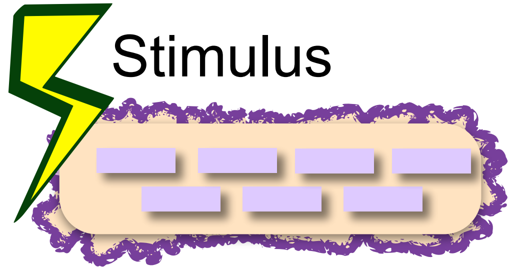

Cardiomyocytes, the cardiac muscle cells, are excitable: when stimulated by the application of an electrical stimulus, the chemo-electric equilibrium of the cell membrane is broken, thus originating a sequence of events that make the electric potential of the cell rise and then fall. Such phenomenon, known as action potential, is due to the opening and closing of voltage-gated ion channels. The resulting flux of ions across the cell membrane makes the transmembrane potential vary.

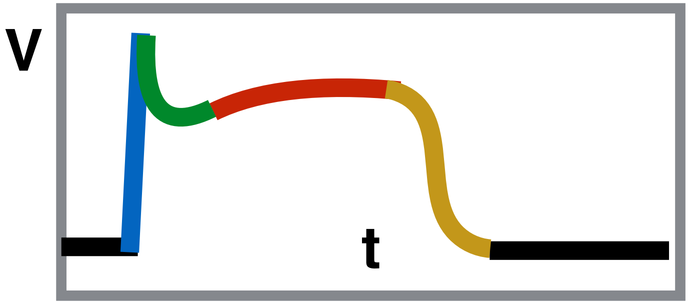

Action potential

1) Depolarization
2) Early repolarization
3) Plateau
4) Repolarization

Calcium ions induce a complex chain of reactions with the final outcome of the generation of active force inside the cardiomyocytes. Finally, the contractile force generated at the microscale causes the macroscopic contraction of the heart chambers.

Cardiac Mechanics

To characterize both its active and passive behavior

the tissue is typically modeled (defined) as an orthotropic material, in particular by accounting for the presence of muscle fibers and collagen sheets.

The Holzapfel-Ogden constitutive law is used, together with the active strain or active stress approach for the activation

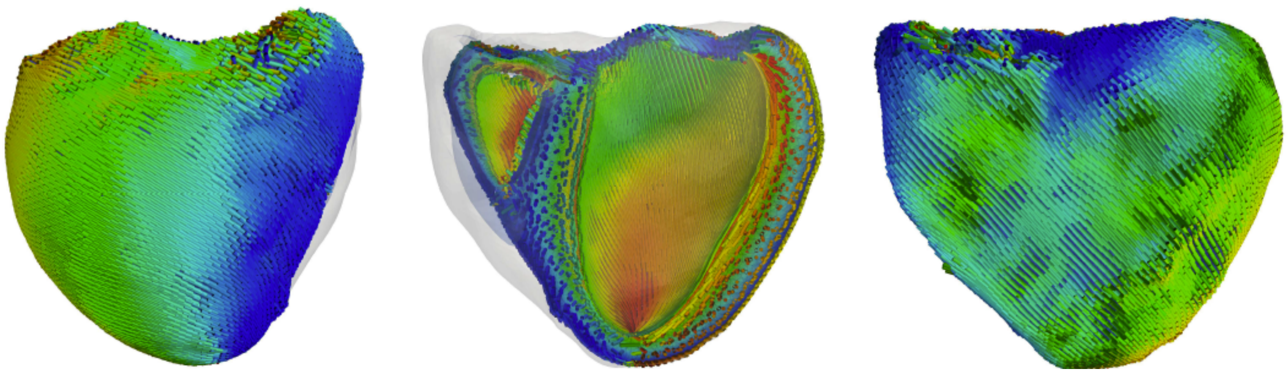

fibers

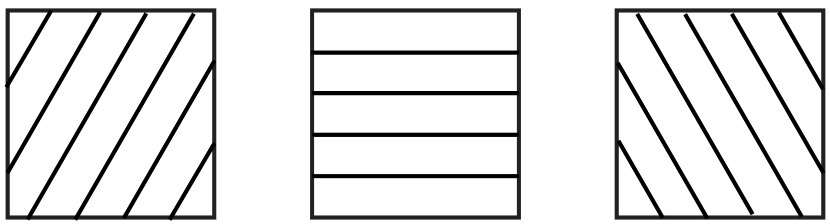

at endocardium at epicardium

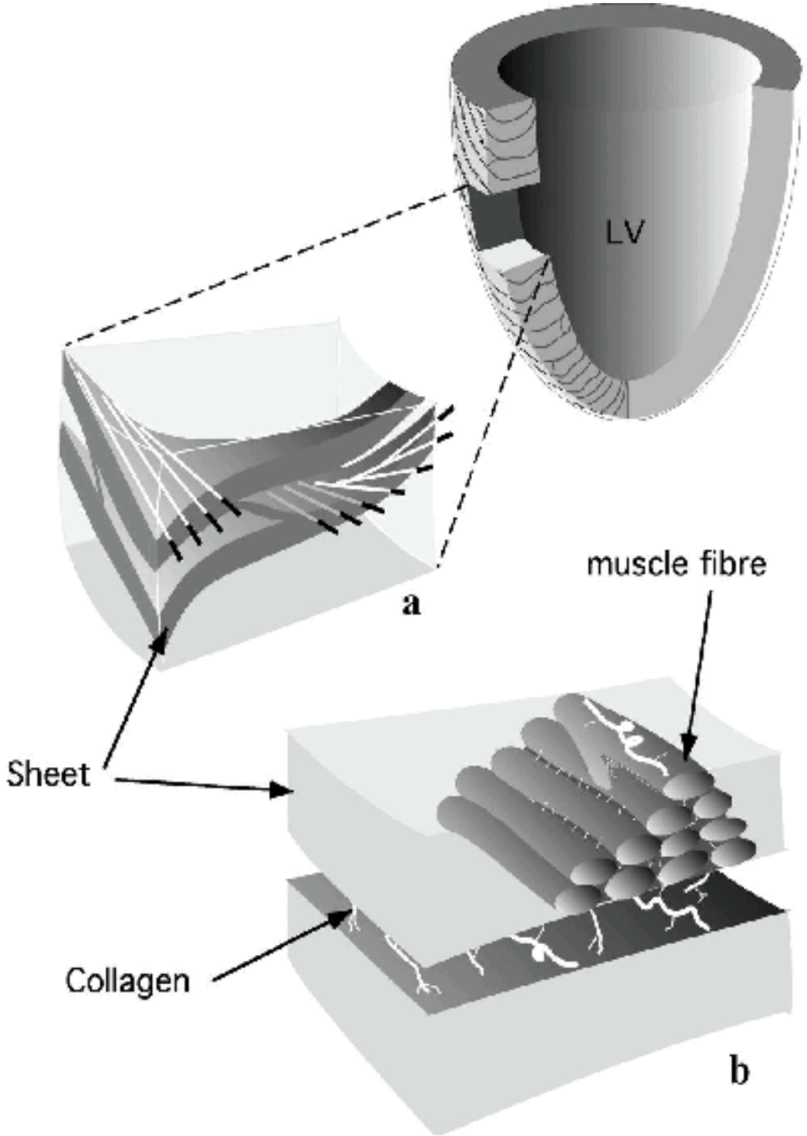

[LeGrice et al. 1995]

Core Cardiac Models

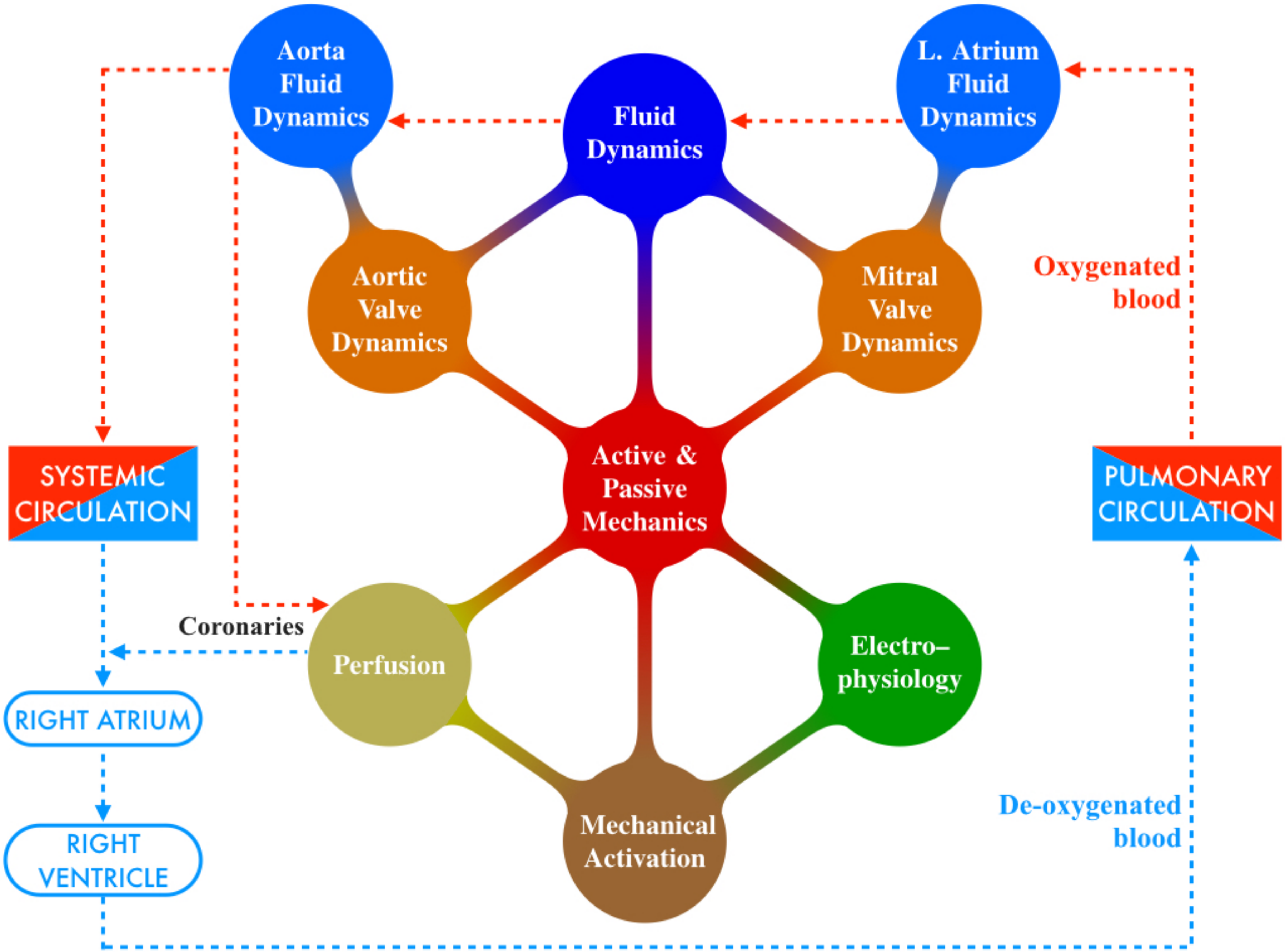

The Mathematical Heart

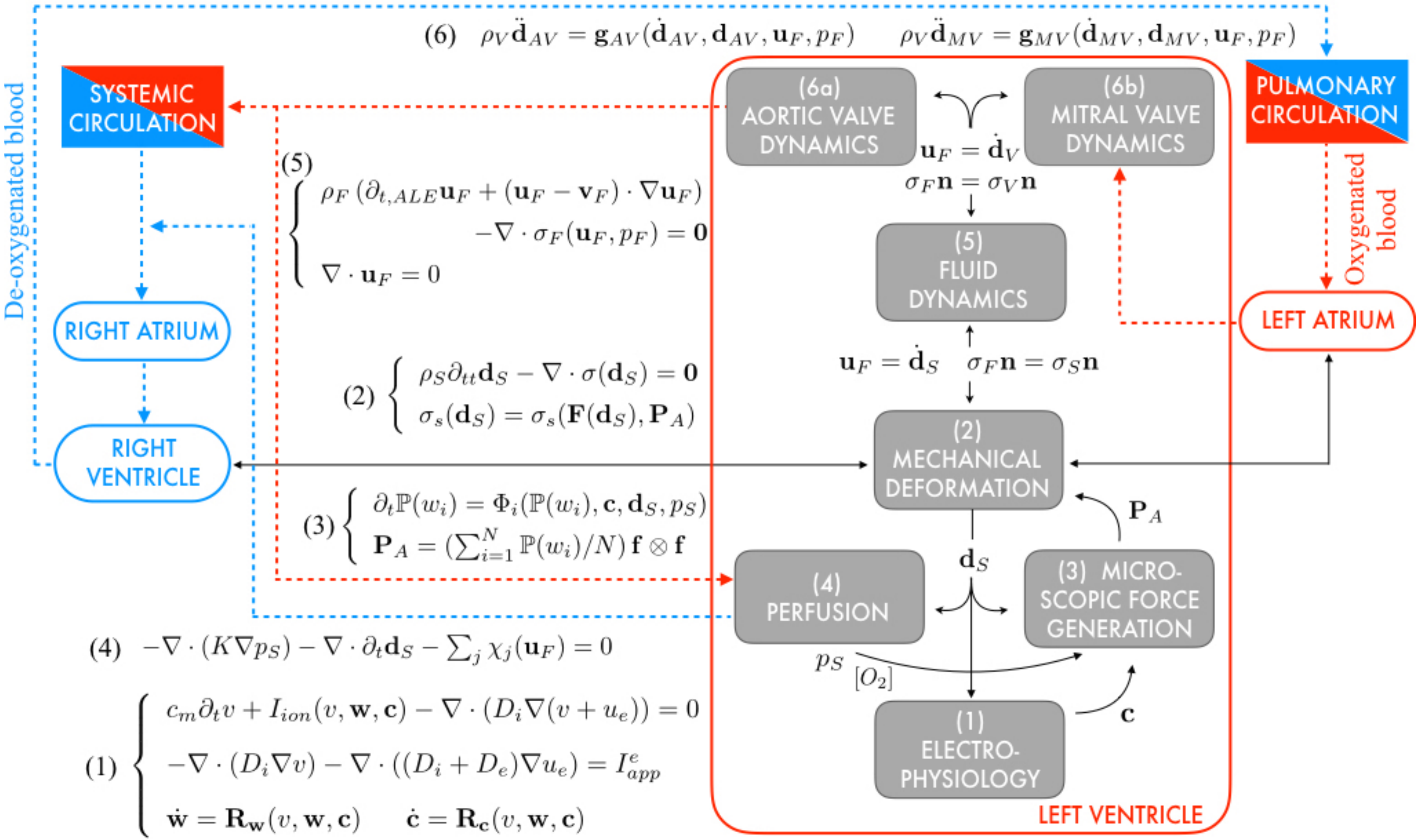

Fibers - Red@Epi Blue@Endo

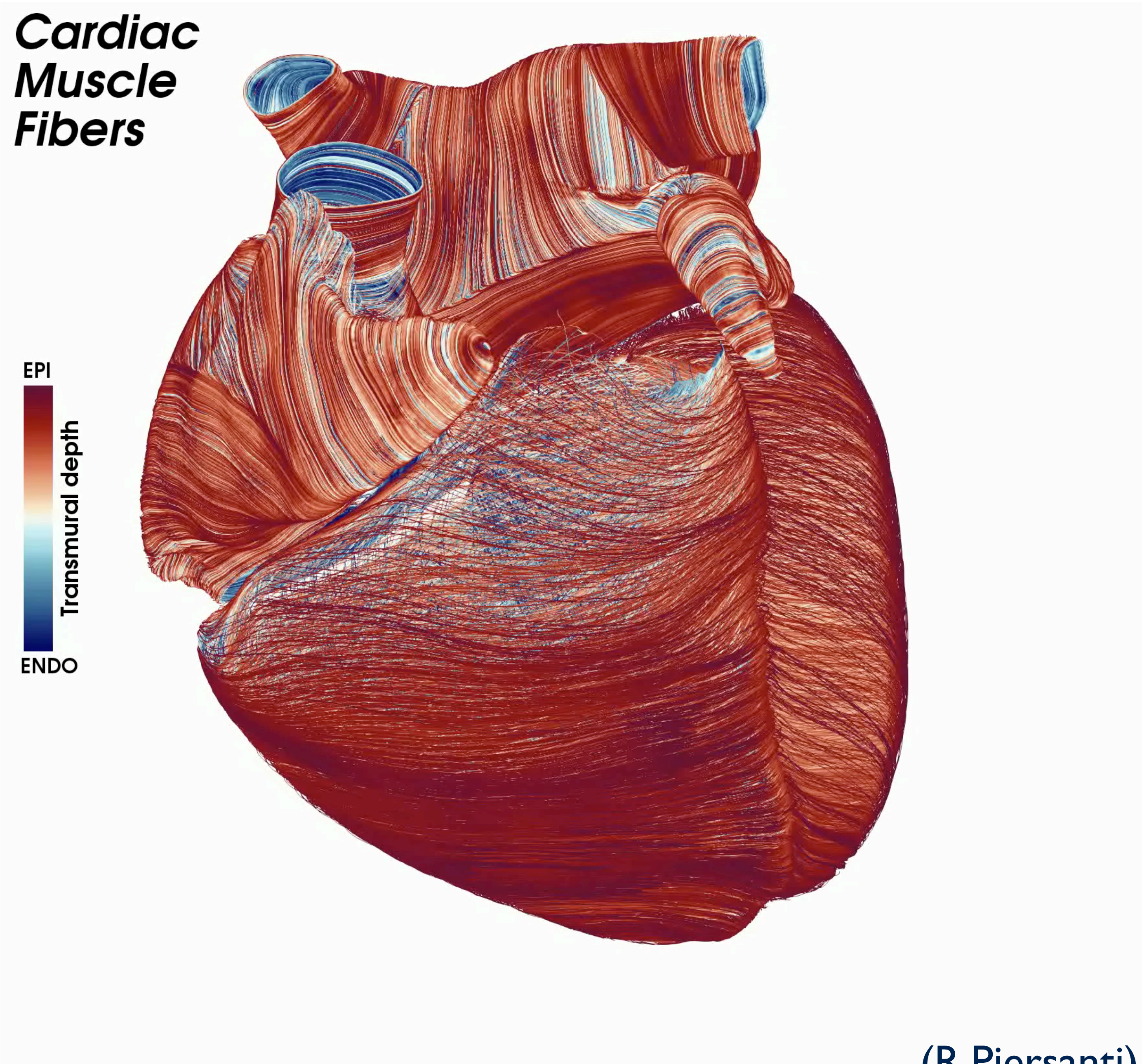

(R.Piersanti)

Longitudinal Section (left), Cross Section (right)

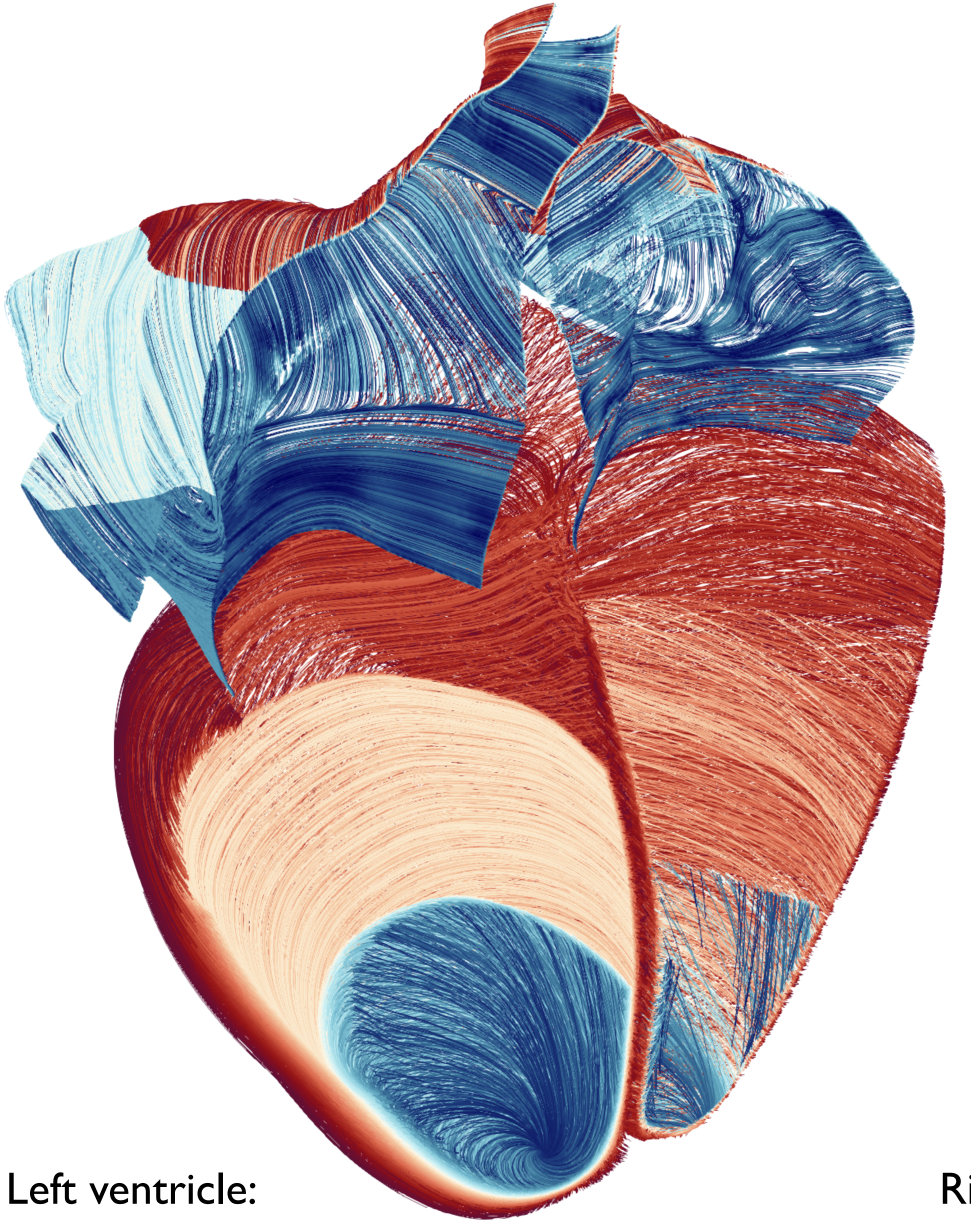

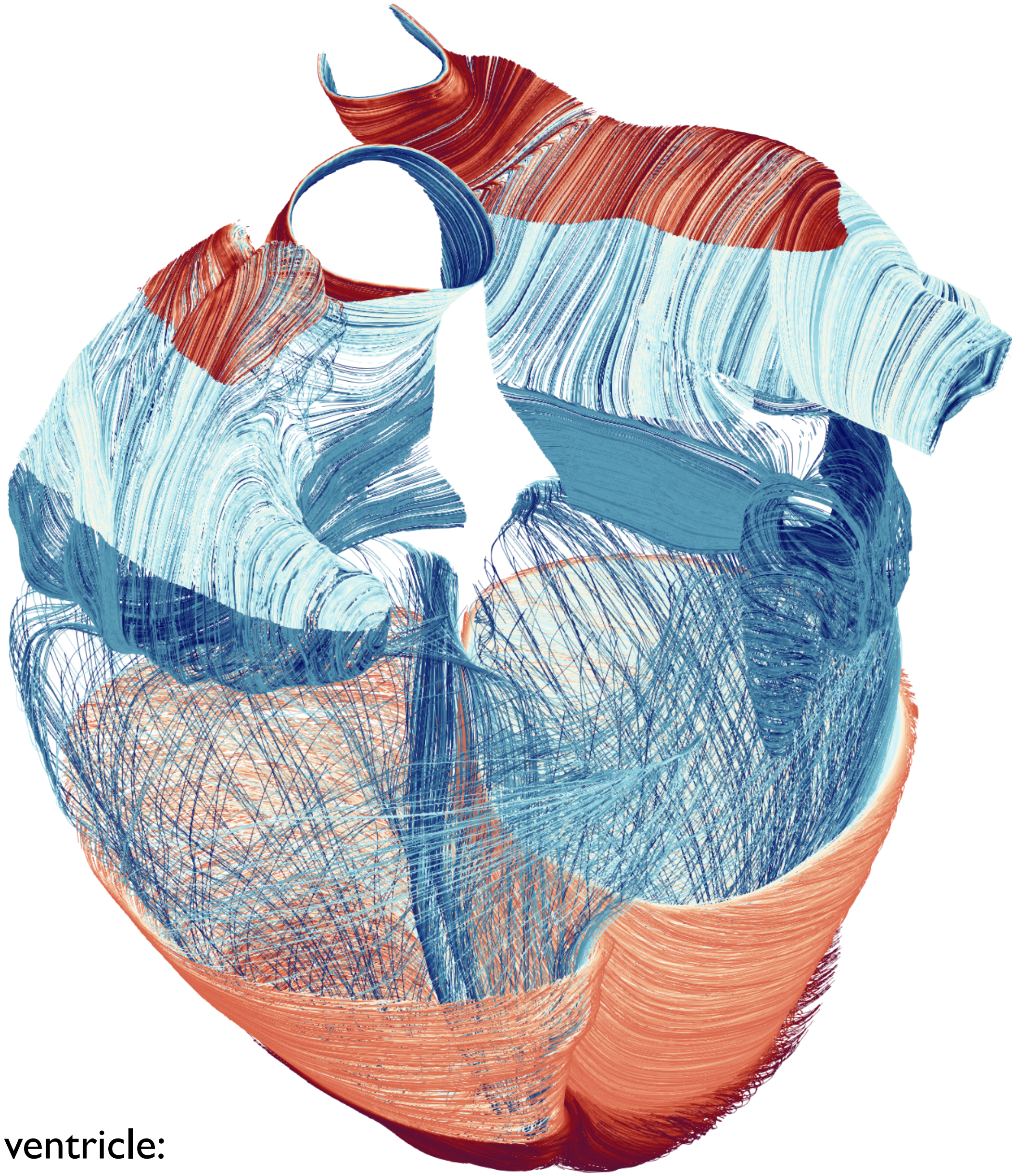

Left ventricle:
Fibers: alpha_endo = +60° alpha_epi = -60°
Sheets: beta_endo = +20° beta_epi = -20°

Right ventricle:
Fibers: alpha_endo = +90° alpha_epi = 0°
Sheets: beta_endo = +20° beta_epi = -25°

Computational mesh with different resolution

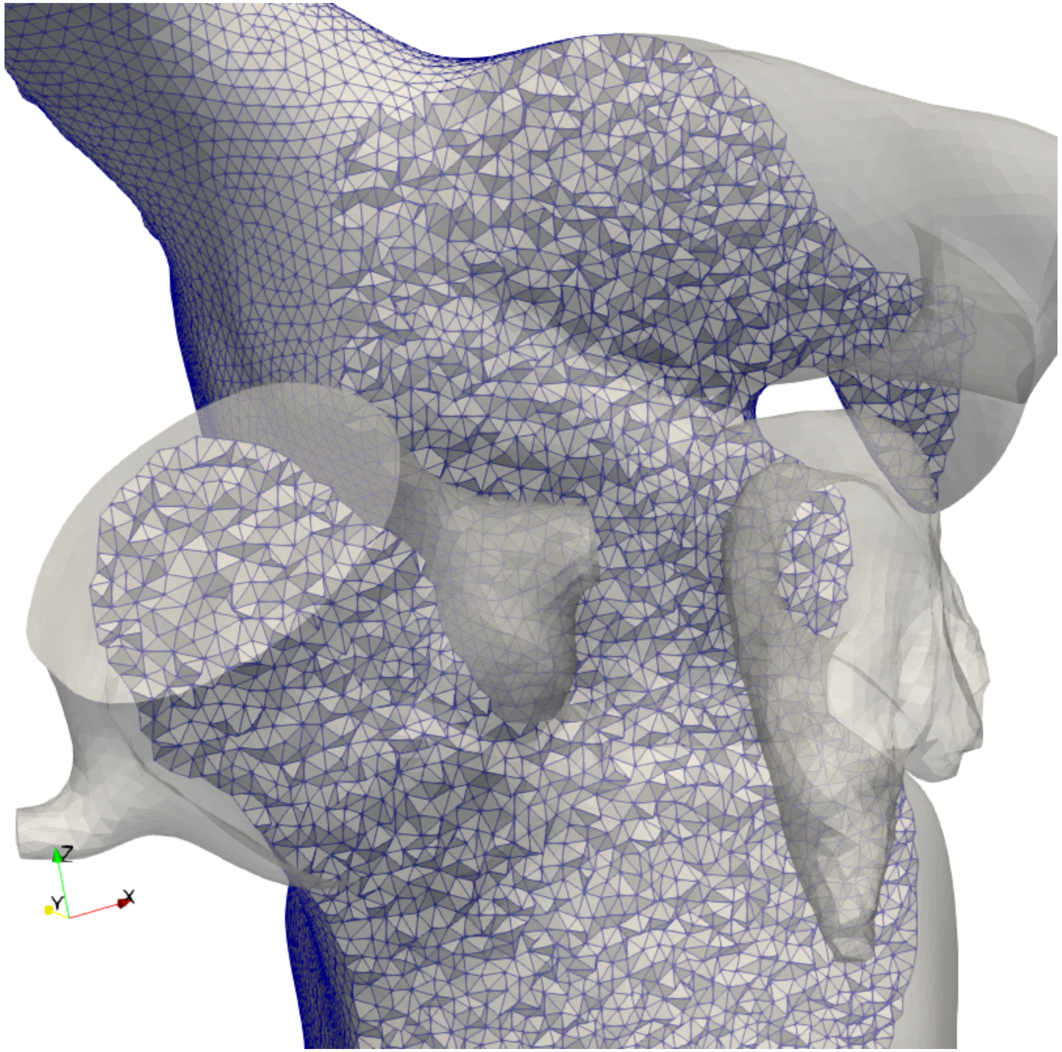

800.000 Elements

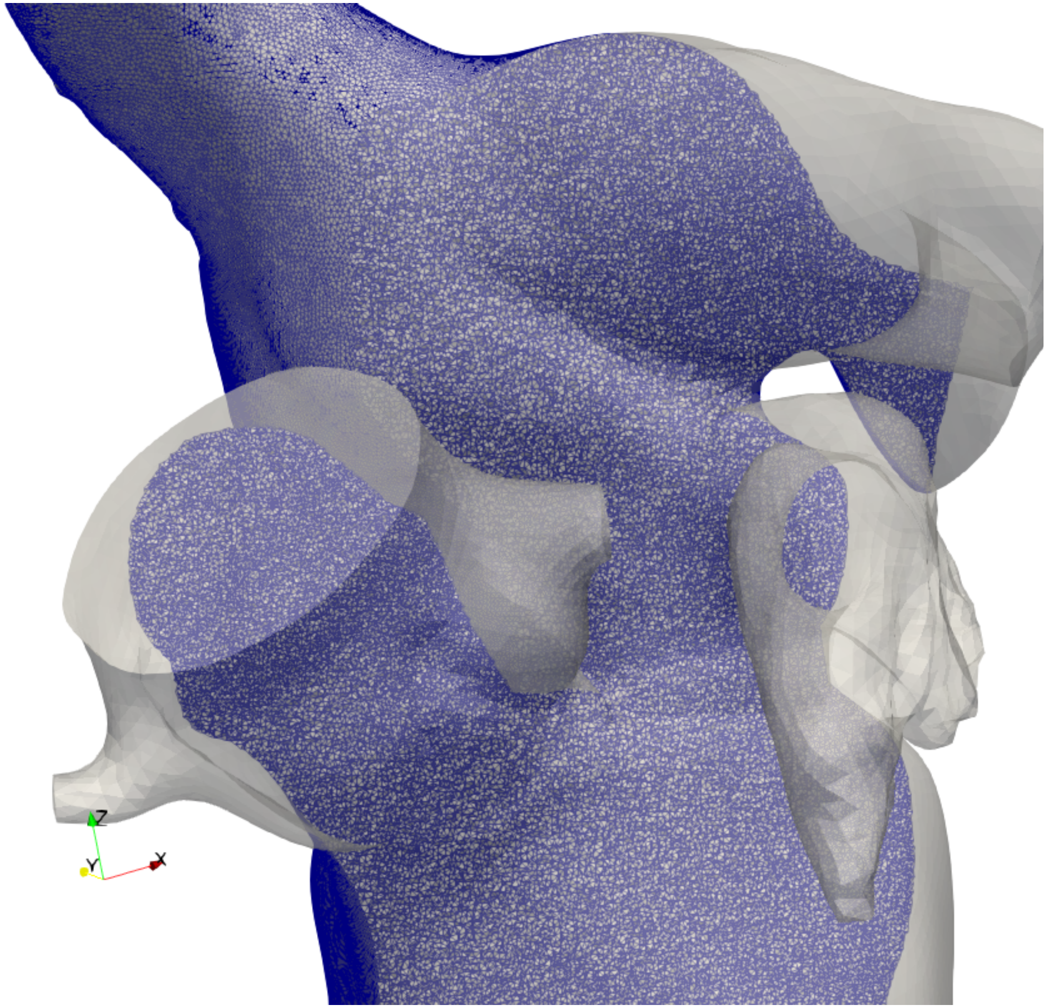

22.000.000 Elements

Finer meshes involve higher computational resources,
however they allow a more accurate numerical solutions

Details matter

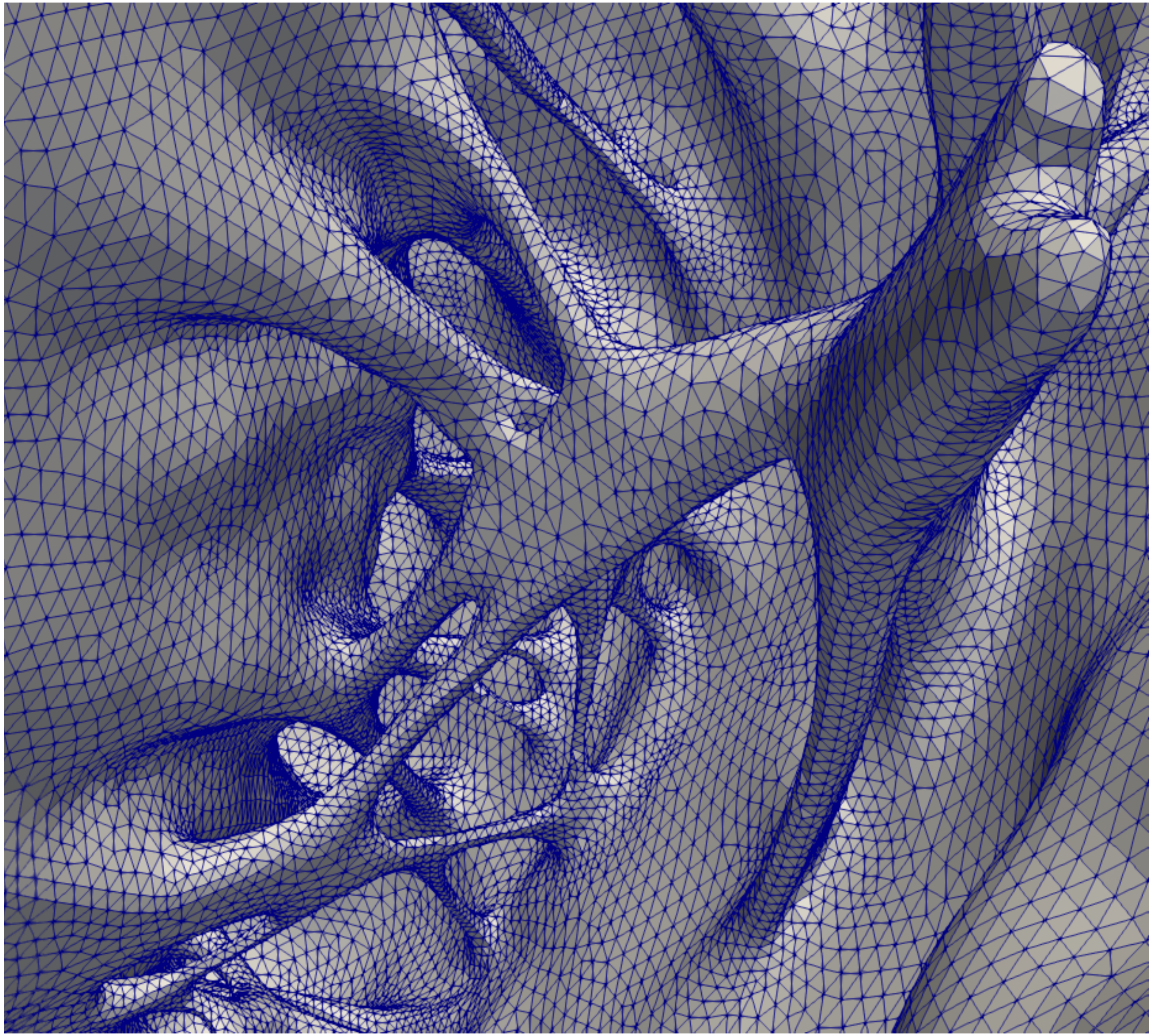

Mesh for papillary muscles and trabeculae carneae in the right ventricle (M.Fedele)

Electric Wave Propagation in the Whole Heart (R.Piersanti)

Time=0 corresponds to the onset on the initial electric stimulus at sino-atrial node (right atrium)

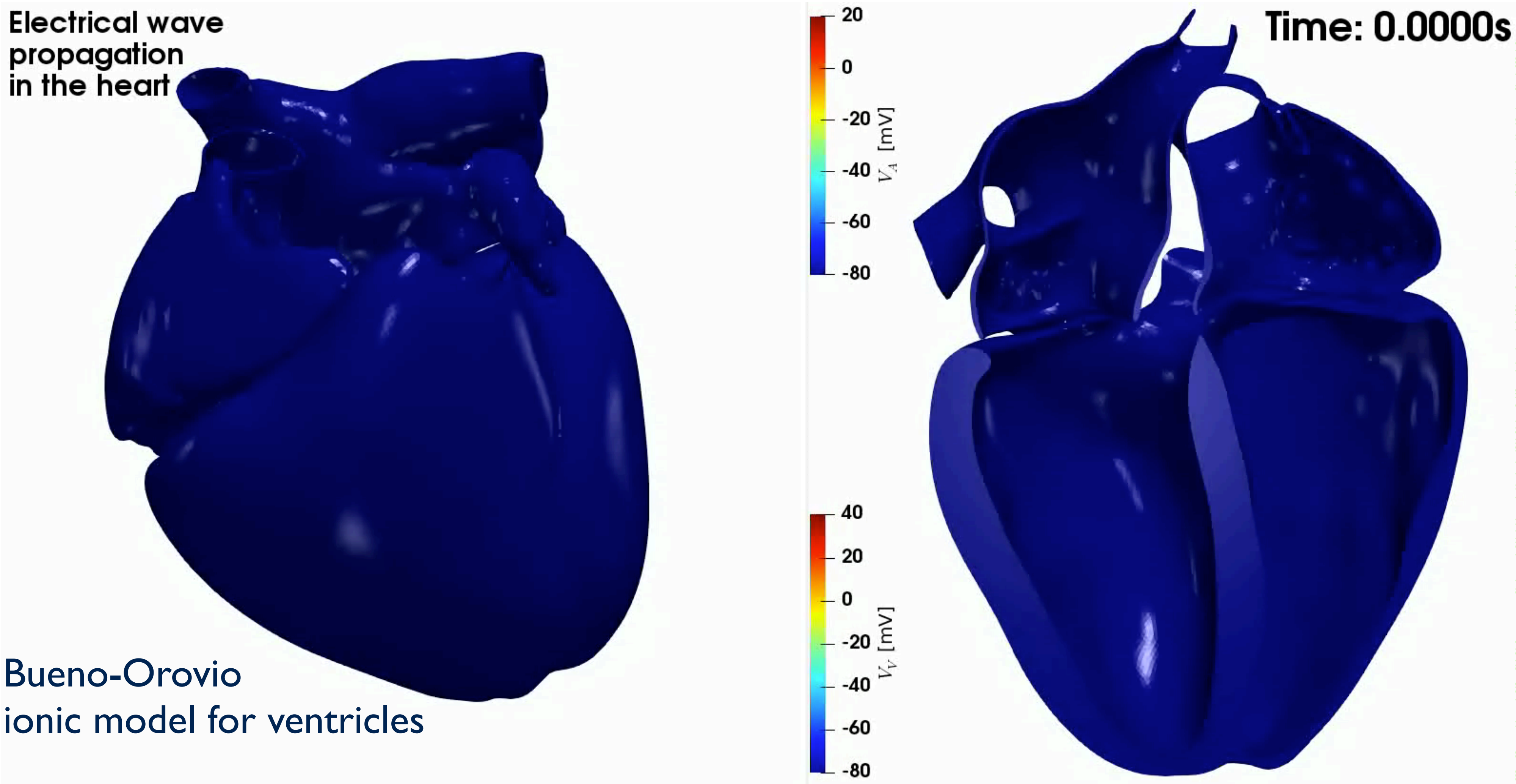

Bueno-Orovio
ionic model for ventricles

Aliev-Panfilov ionic model for atria

Monodomain semi implicit scheme with respect to I_ion
BDF2 in time; FEM P1 in space; # dof: 1.2M tetrahedra
h = 1mm dt = 0.05 ms

Atrial Fibrillation (AF) is the most common type of **cardiac arrhythmia**.

AF is a condition in which heart electrical signal propagates in a rapid and irregular way throughout the atria

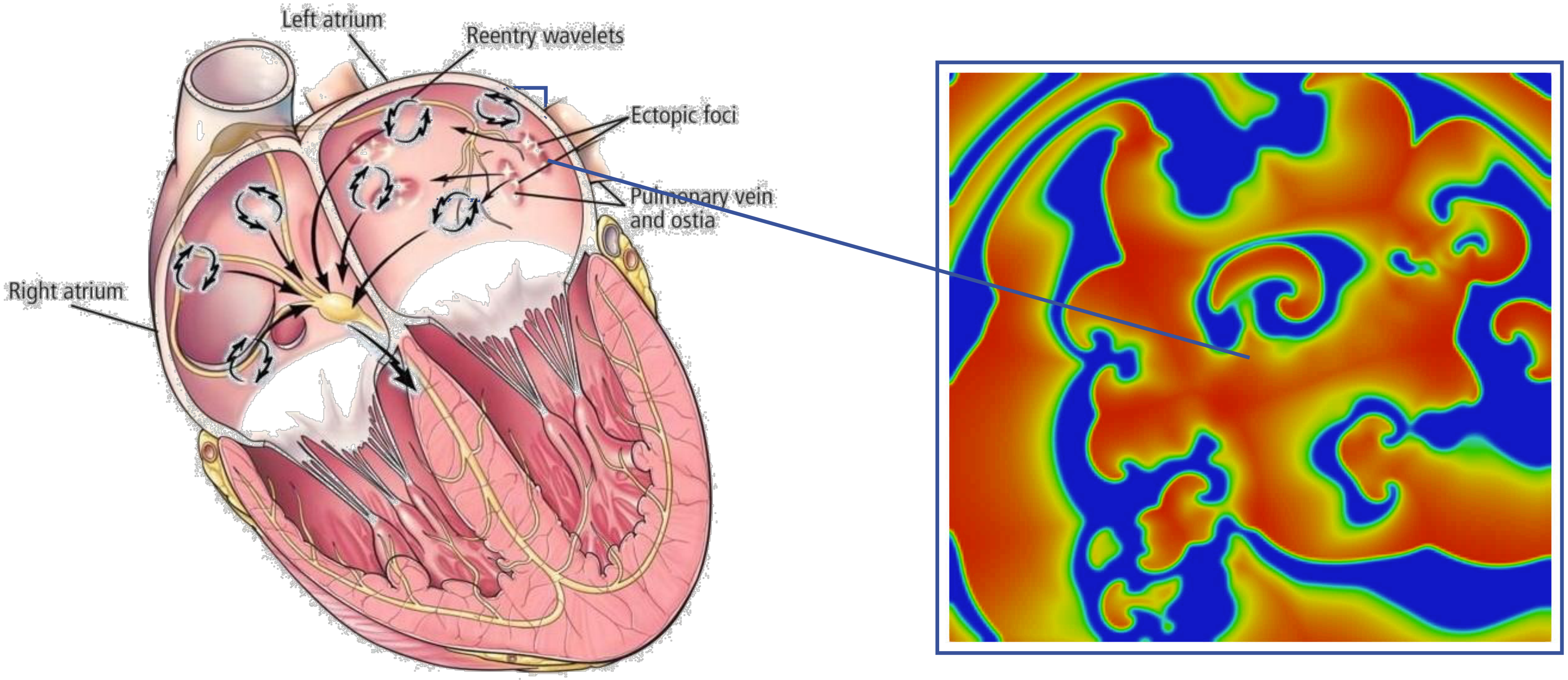

- During AF, atrial cells fire at rates of 200-600 times per minute.
- AF causes substantial **morbidity** and an increase of mortality

Figure of eight re-entry

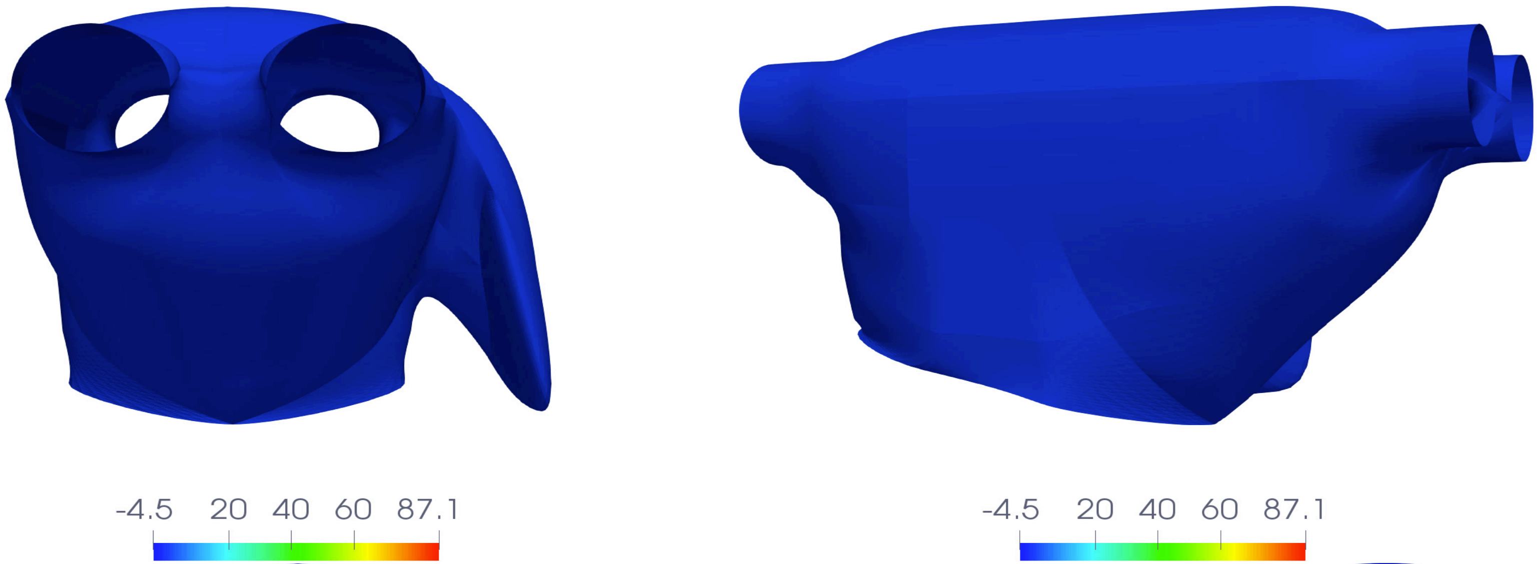

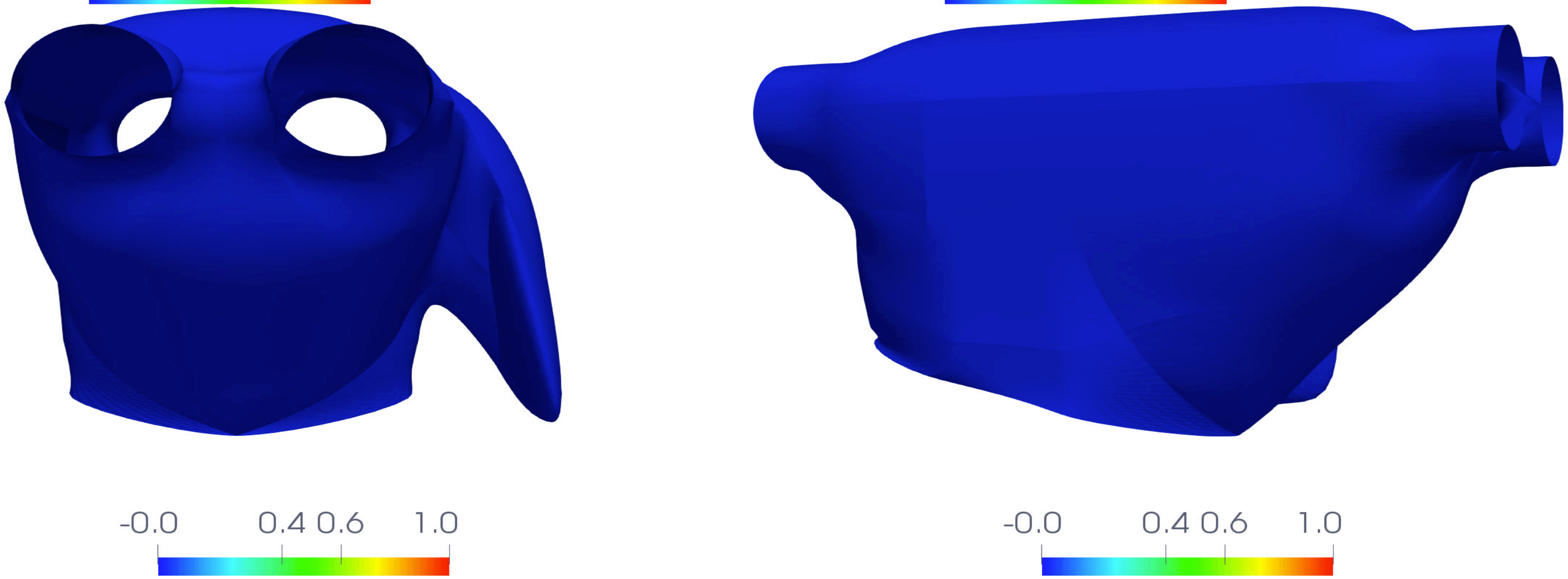

Re-entry break-up

Solutions obtained through **P2/C1 NURBS-based IGA** with N = 61732 and **BDF2 semi-implicit** scheme.

We reproduce the PV loops for studying scenarios with different sizes of the necrotic regions ("small", "medium", and "large").

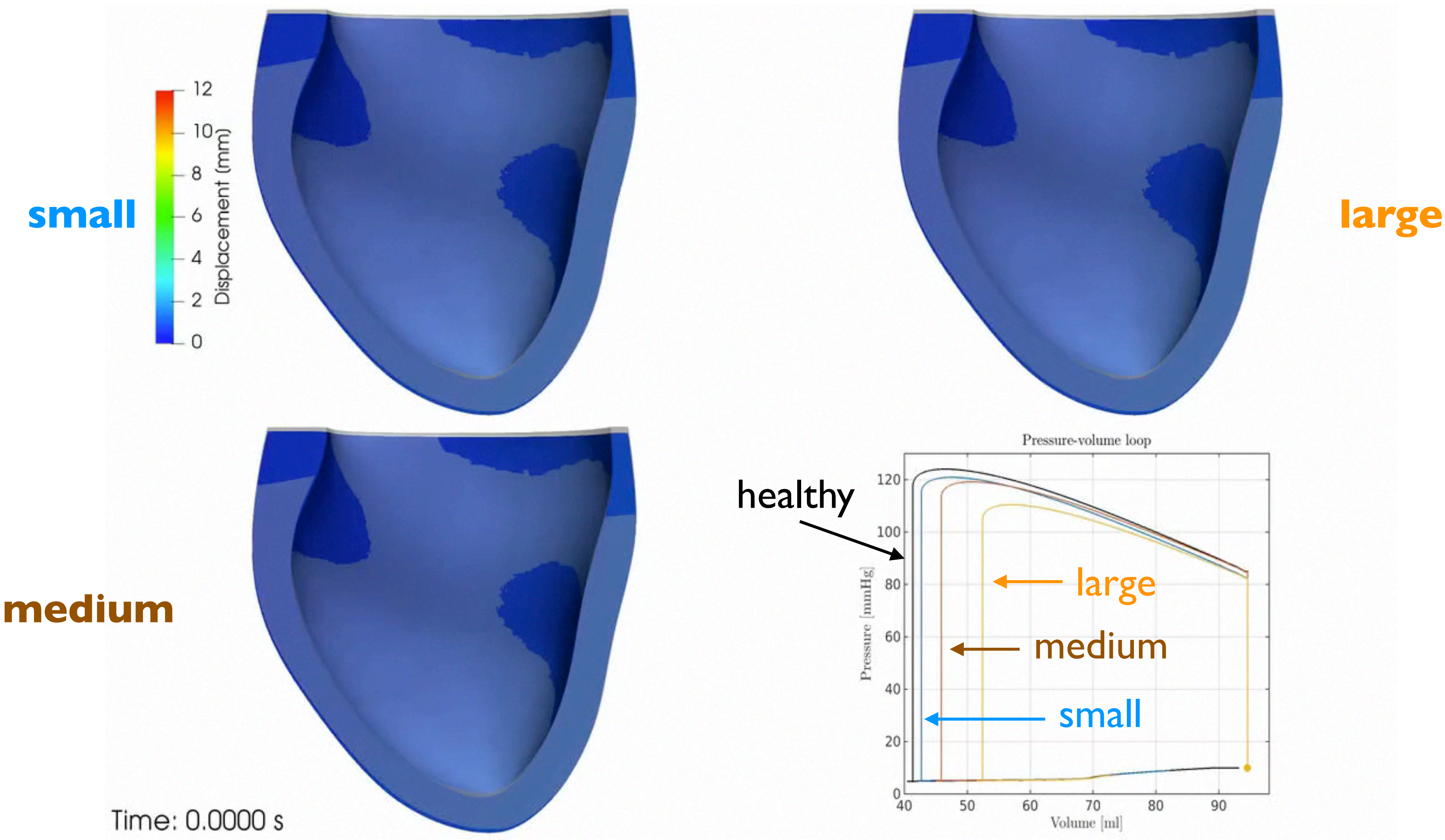

A Full Heartbeat in Left Atrium - Streamlines (A.Zingaro)

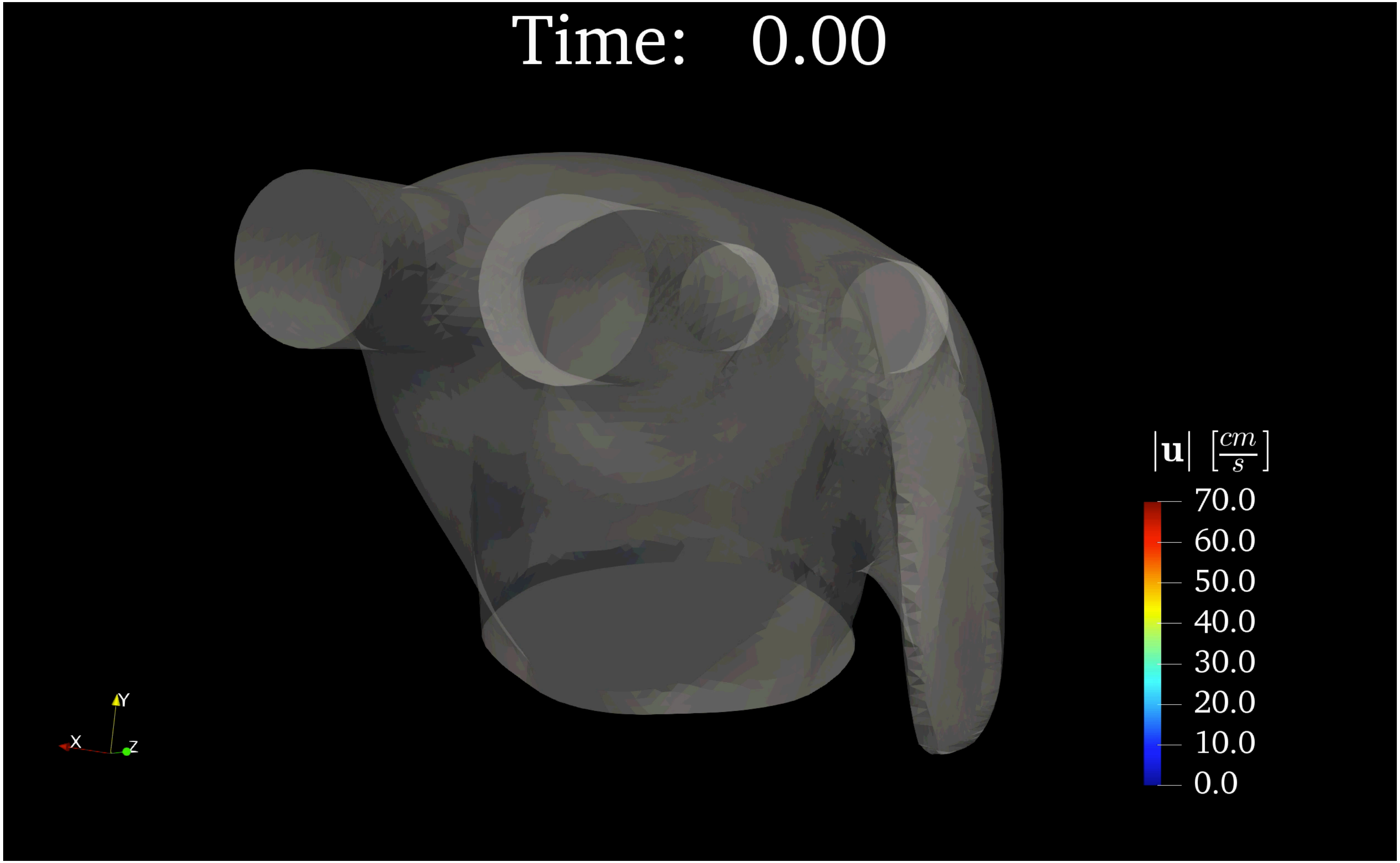

ALE-NS with VMS-LES; h=1mm, Dt=0.005s; diastole 0.-0.68s, systole 0.68-1.s
switching by Neumann to Dirichlet B.C. on mitral valve; auricula on front-right

Atrioventricular flow (left heart) (F. Menghini)

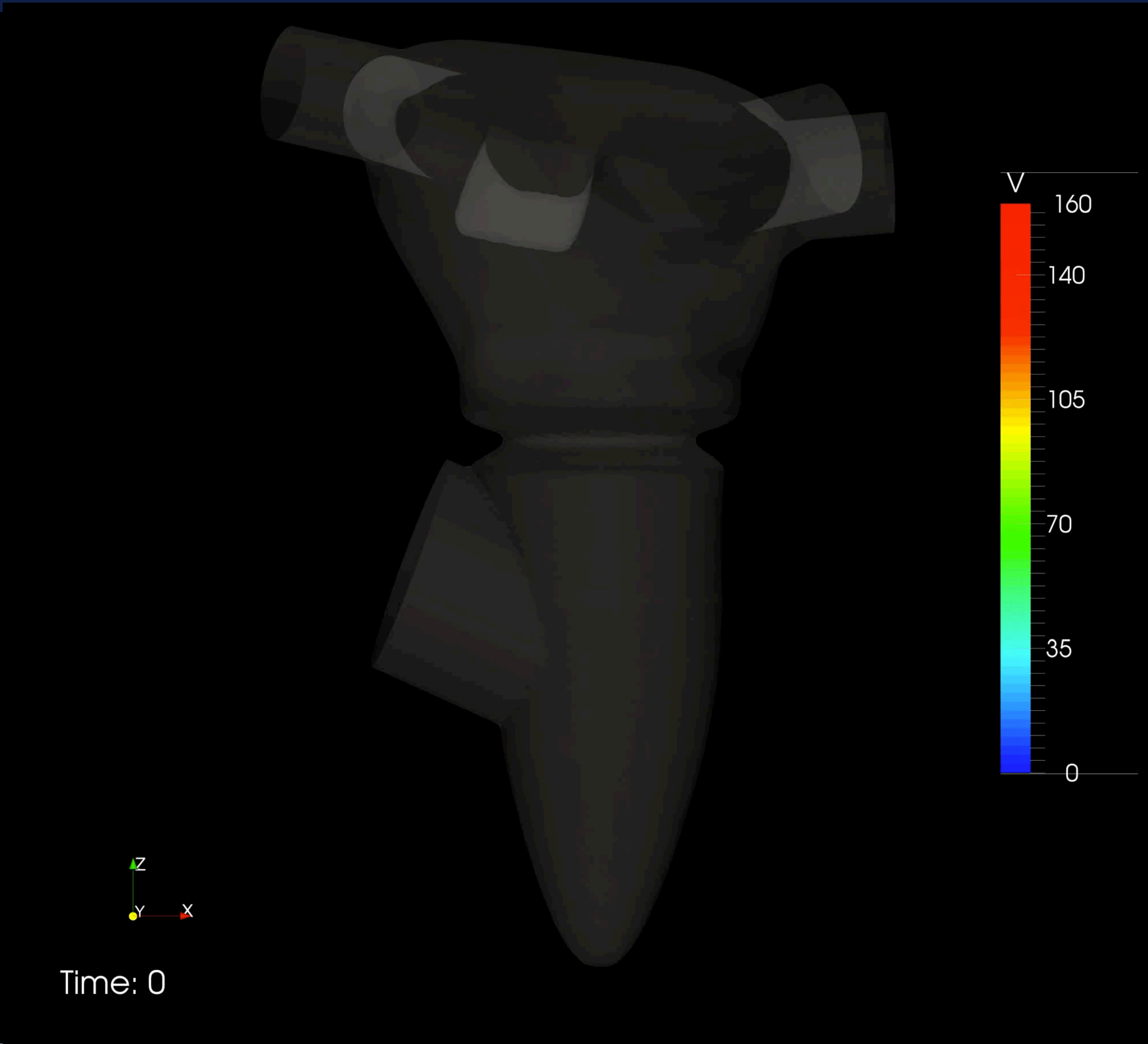

Atrioventricular flow (left heart): Q criterion (F. Menghini)

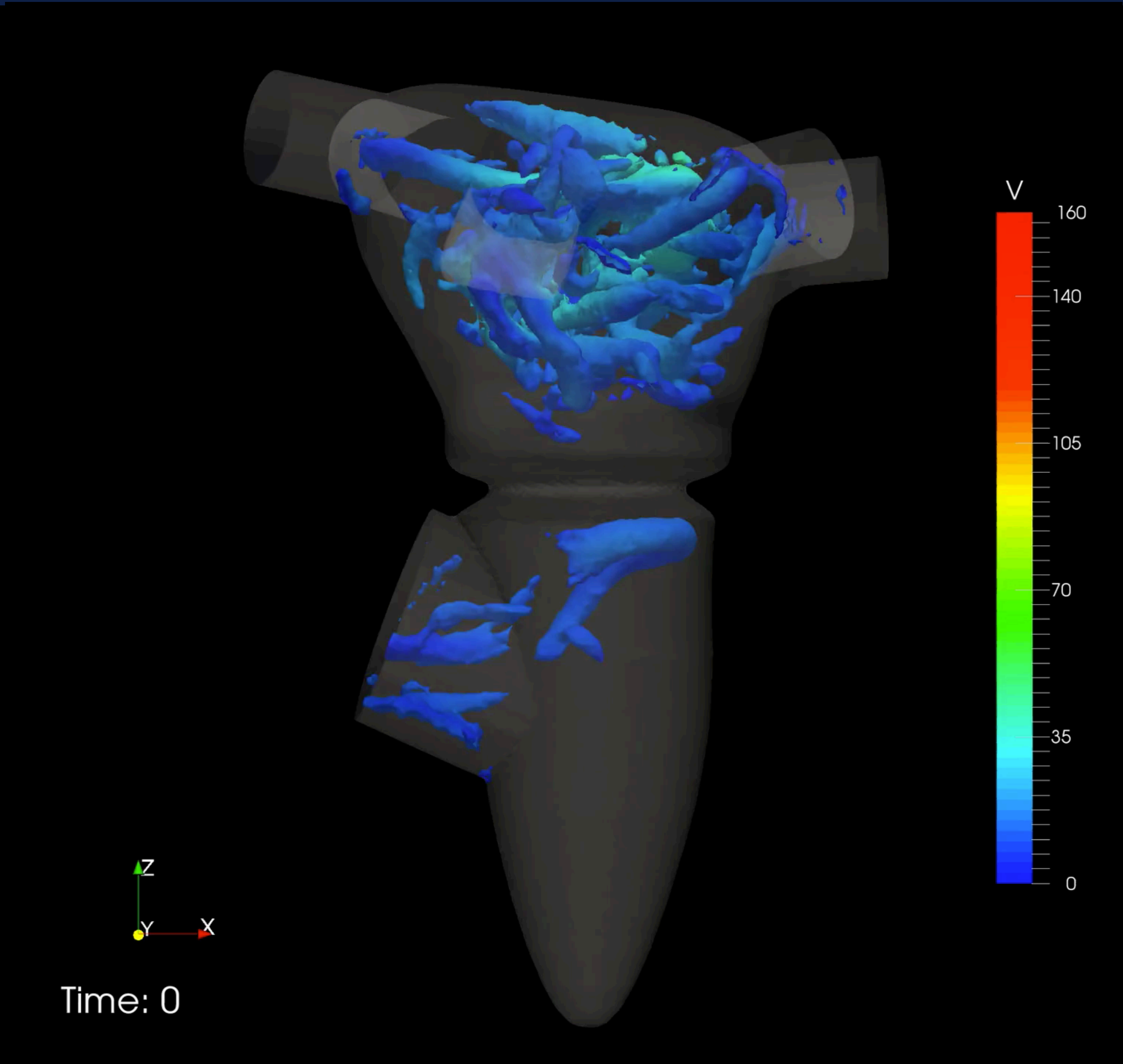

Velocity, pressure on the leaflets, pathlines, & particles residency time

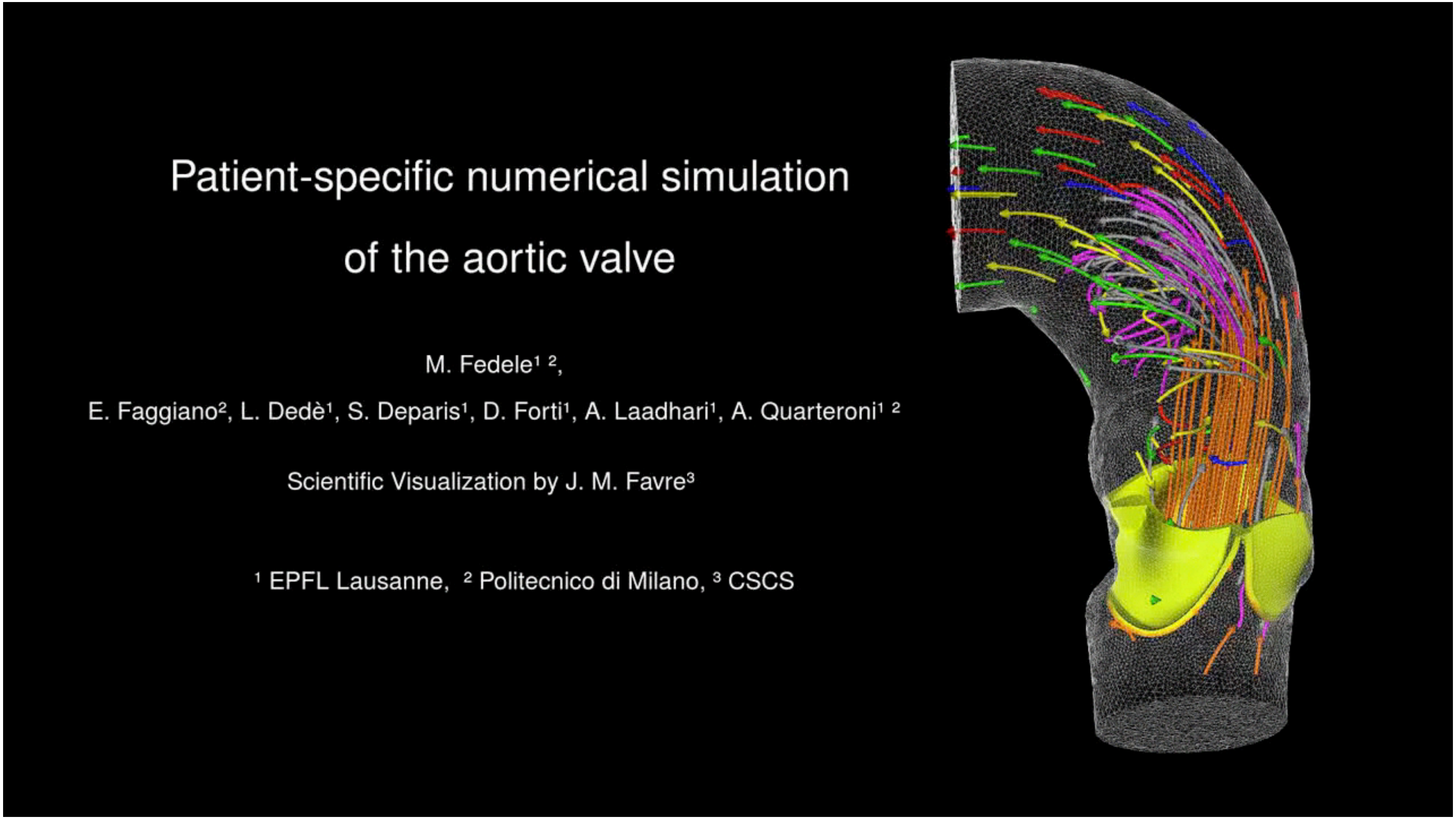

VMS-SUPG stabilization, P1-P1 FEM, BDF2

Accounting for Variability (and Uncertainty)

Accounting for Uncertainty

Major challenges facing cardiac modelling include parameter inference from uncertain experimental measurements, model personalisation to patient date, model selection, model discrepancy from reality, and the way these factors affect the confidence in model prediction

Epistemic uncertainty

Lack of knowledge (didn't measure it)
Experimental error (didn't measure it correctly)

Aleatory uncertainty

Stochasticity (an individual reacts differently each time: intrinsic)
Variability (between individuals: extrinsic)

Two different fiber angles - effect on displacement

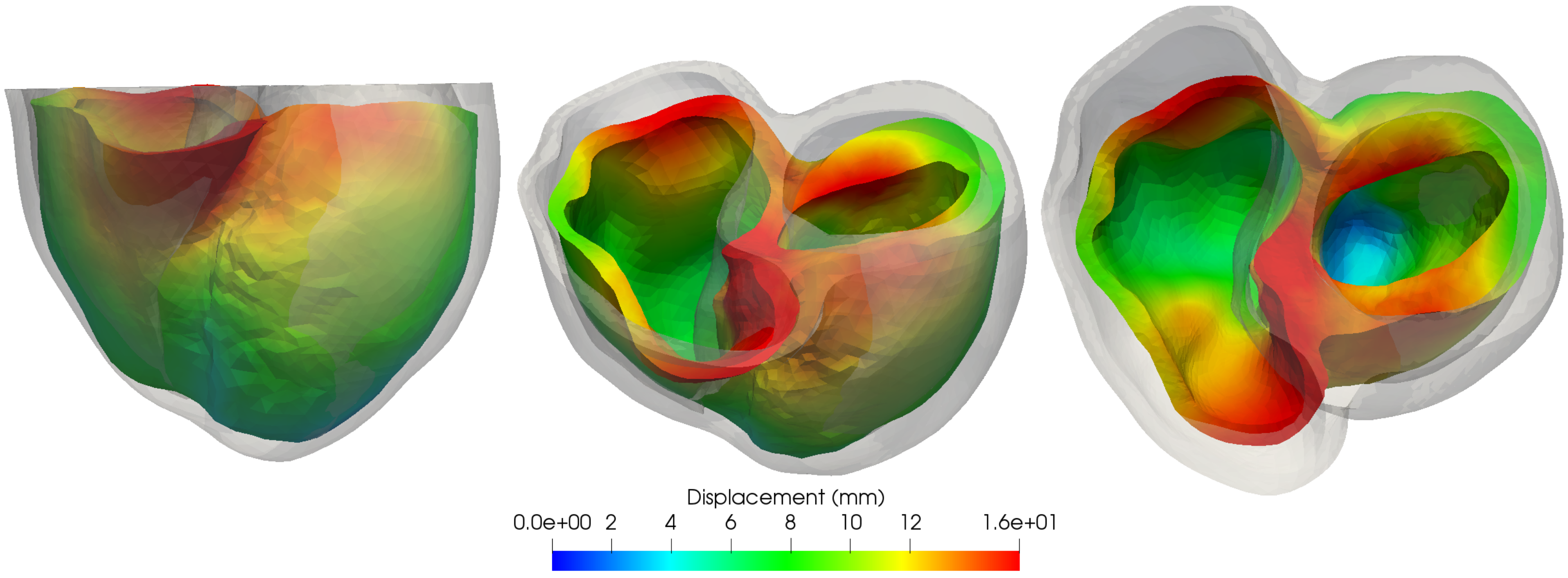

(a)

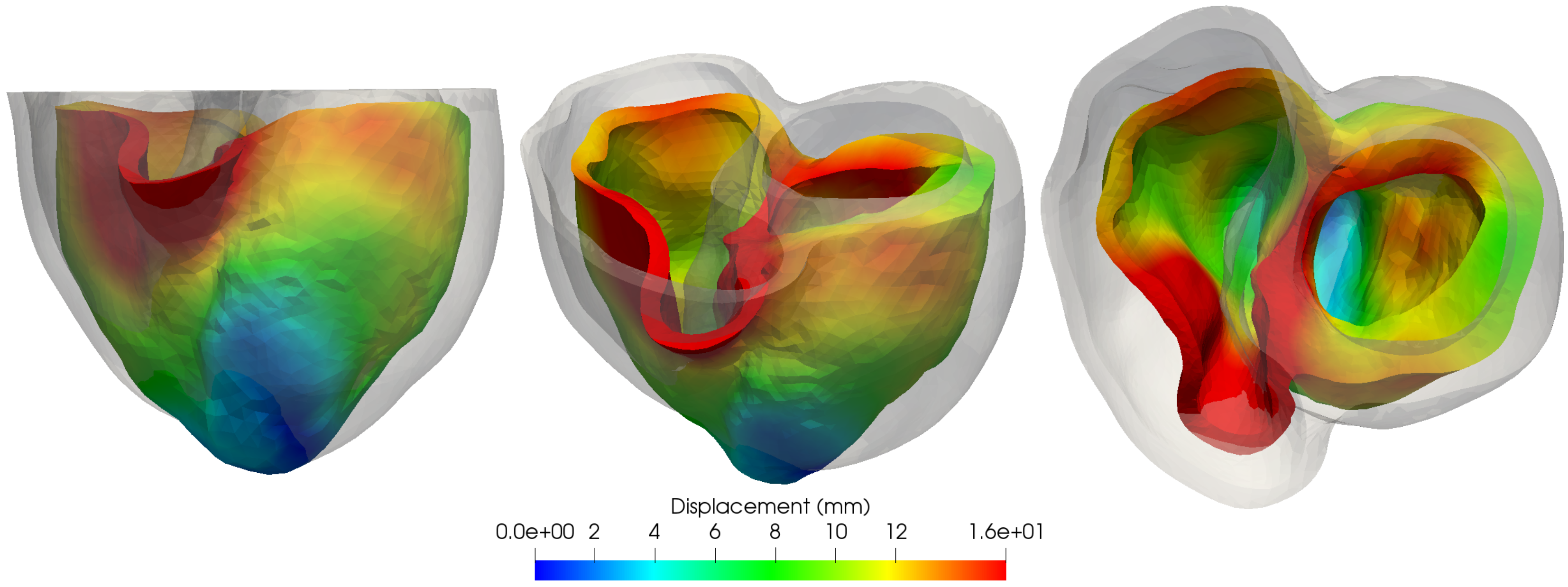

(b)

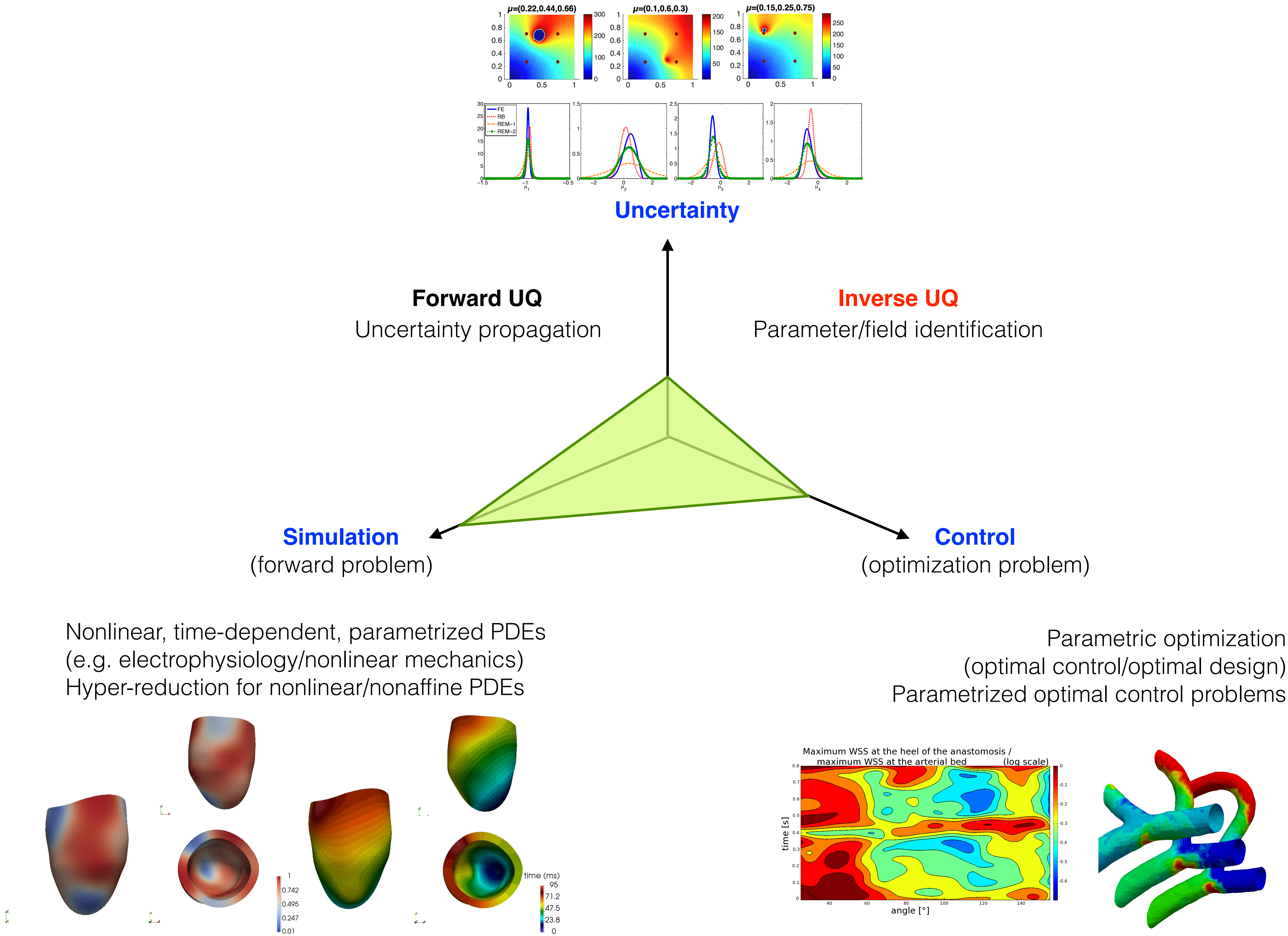

μ=(0.22,0.44,0.66)
μ=(0.1,0.6,0.3)
μ=(0.15,0.25,0.75)
FE
RB
REM−1
REM−2
Uncertainty
Forward UQ
Uncertainty propagation
Inverse UQ
Parameter/field identification
Simulation
(forward problem)
Control
(optimization problem)
Nonlinear, time-dependent, parametrized PDEs
(e.g. electrophysiology/nonlinear mechanics)
Hyper-reduction for nonlinear/nonaffine PDEs
Parametric optimization
(optimal control/optimal design)
Parametrized optimal control problems
time (ms)
Maximum WSS at the heel of the anastomosis /
maximum WSS at the arterial bed
(log scale)
time [s]
angle [°]

One Week *

for

One Second

*** Pizz Daint (27 petaflop)**

Reduced-order models

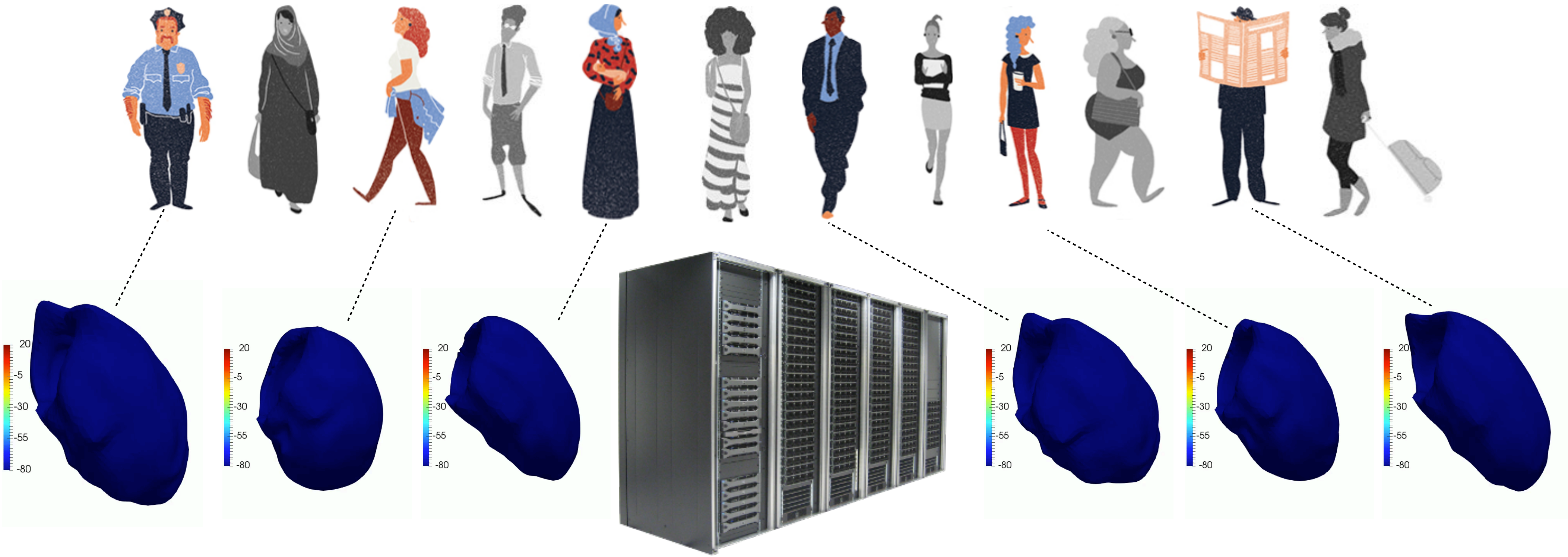

Projection

New subject

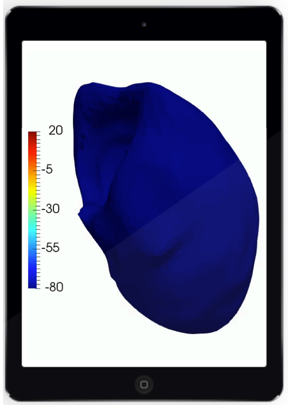

TOOLS:

Reduced basis method

proper orthogonal decomposition

hyper reduction techniques

...

(with A.Manzoni & S.Pagani)

AIM

Better understanding of physiology (quantitative analysis)

Supporting clinical decision-makings

Help designing optimal surgical operations

FEATURES

Non-invasive

Accurate

Reliable

Inexpensive (research apart)

Myocardial Perfusion

The **myocardial perfusion** is the delivery of blood to the heart muscle, named *myocardium*, supplied by the *coronary circulation*

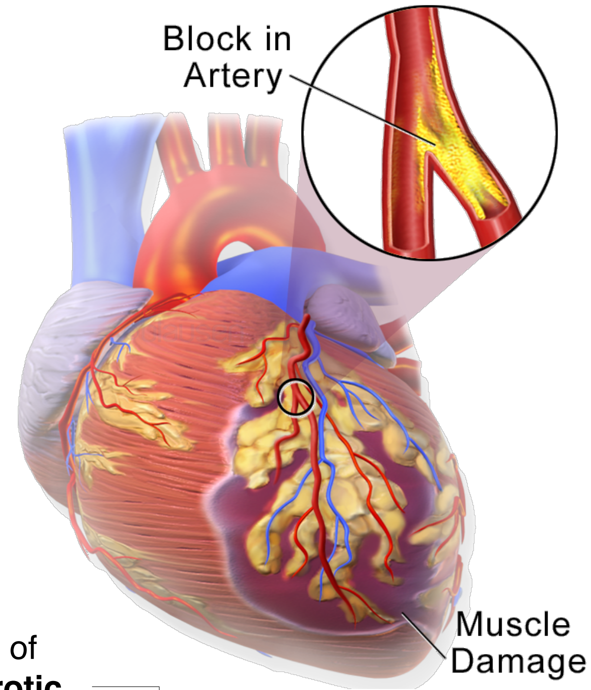

Formation of **atherosclerotic plaques**

Coronary vessel **occlusion**

Myocardial **Ischemia**

Tissue **Necrosis** and **Scar** Formation

➢ First cause of death in western countries (36% in 2010) *[Herrington et al. 2016]*

Multiscale modeling approach

Epicardial Vessels: **3D Navier-Stokes Equation**

Interface Conditions

Intramural Vessels: **Multi-Compartment Darcy Model**

Homogeneization

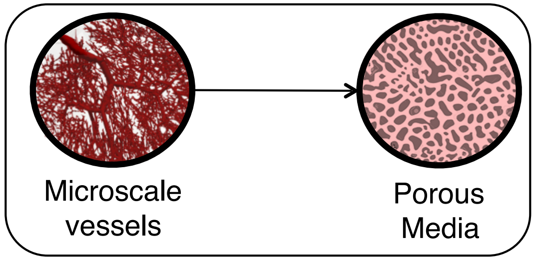

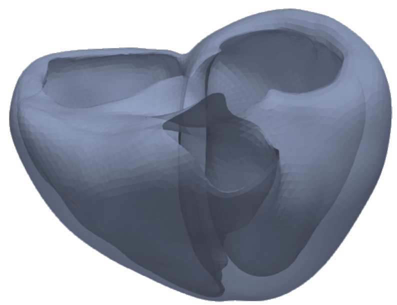

A collaboration with: Dott. G. Pontone

Centro Cardiologico Monzino

A Three Compartment Model

Epicardial Vessels: **3D Navier-Stokes Equation**

$$\rho\left(\frac{\partial \boldsymbol{u}_C}{\partial t} + (\boldsymbol{u}_C \cdot \nabla)\boldsymbol{u}_C\right) - \mu\nabla \cdot \left(\nabla \boldsymbol{u}_C + (\nabla \boldsymbol{u}_C)^T\right) + \nabla p_C = \mathbf{0} \qquad \text{in } \Omega_C,$$

$$\nabla \cdot \boldsymbol{u}_C = 0 \qquad \text{in } \Omega_C$$

$\boldsymbol{u}_C$ coronary blood velocity
p_C coronary blood pressure
ρ blood density
μ blood viscosity
Γ_{out} terminal outlet

Intramural Vessels: **Multi-Compartment Darcy Model**

To capture the **different length scales** of the intramural vessels (radius from 300 to 8 μm)

3 Darcy compartments **co-existing** in the same domain

$$K_i^{-1}\boldsymbol{u}_i + \nabla p_i = 0 \qquad \text{in } \Omega_M,$$

$$\nabla \cdot \boldsymbol{u}_i = \sum_{k=1}^{3} \beta_{i,k}(p_i - p_k) \qquad \text{in } \Omega_M \qquad i = 1 \dots 3$$

+ interface contribution coming from coronaries

$\boldsymbol{u}_i$ Darcy velocity $\quad K_i$ permeability tensor
p_i pore pressure $\quad \beta_{i,k}$ inter-compartment coupling coefficient

$\beta_{i.k}$ and $\boldsymbol{K}_i$ are estimated from a **1D intramural vessel network**

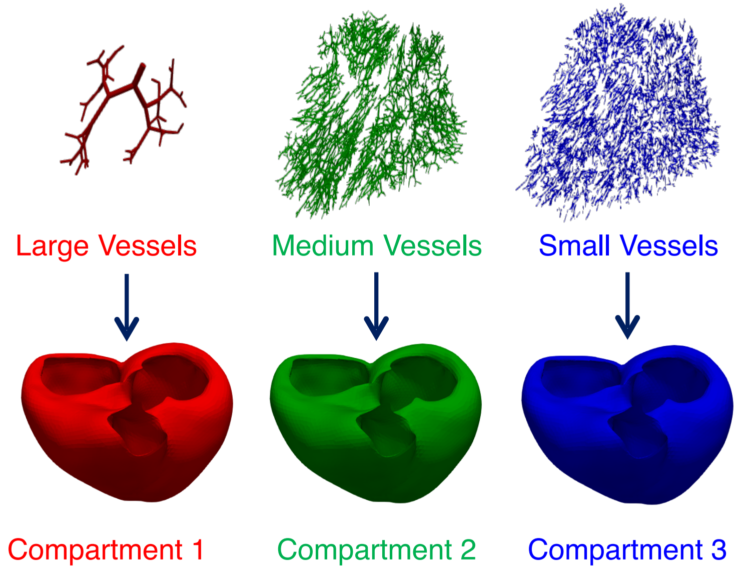

Interface Conditions

Third Newton's Law

based on the hydraulic analog of Ohm's law between coronaries and first compartment

$$p_C - \mu\left(\nabla \boldsymbol{u}_C + (\nabla \boldsymbol{u}_C)^T\right)\boldsymbol{n} \cdot \boldsymbol{n} - \frac{1}{\alpha}\int_{\Gamma_{out}} \boldsymbol{u}_C \cdot \boldsymbol{n}\, d\gamma = \frac{1}{|\Omega_M|}\int_{\Omega_M} p_1(\boldsymbol{x})\, d\boldsymbol{x} \quad \text{on} \quad \Gamma_{out},$$

$$\mu(\nabla \boldsymbol{u}_C + (\nabla \boldsymbol{u}_C)^T)\boldsymbol{n} \cdot \boldsymbol{\tau}_i = 0, \quad i = 1,2 \quad \text{on} \quad \Gamma_{out}$$

Mass Conservation

$$\nabla \cdot \boldsymbol{u}_1 = \frac{1}{|\Omega_M|}\int_{\Gamma_{out}} \boldsymbol{u}_C \cdot \boldsymbol{n}\, d\gamma - \sum_{k=1}^{3} \beta_{1,k}(p_1 - p_k) \quad \text{in } \Omega_M$$

Myocardial perfusion: evolution of the blood pressure

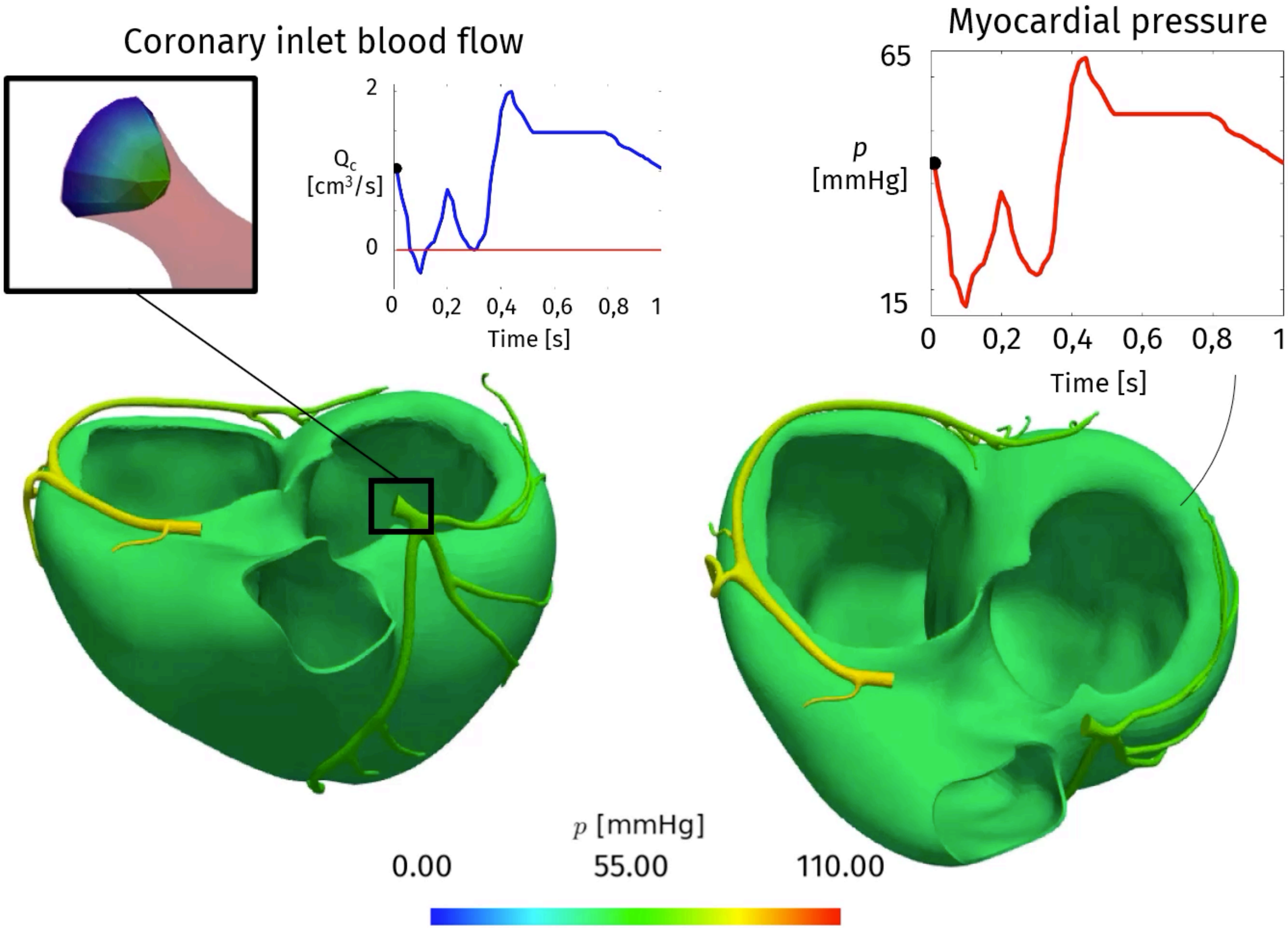

Different coronary by-passes (with R. Scrofani, Ospedale Sacco Milano)

Aim of the computational study:

Comparison of the performance between radial artery (RA) and saphenous vein (SV)
(Guerciotti,Vergara,Ippolito,Quarteroni,Antona,Scrofani,Medical Engineering&Physics, 2017)

3 patients (P1,P2,P3), 2 with RA and 1 with SV

For each of them we virtually design the alternative by-pass (in red)

Fluid-structure interaction simulations

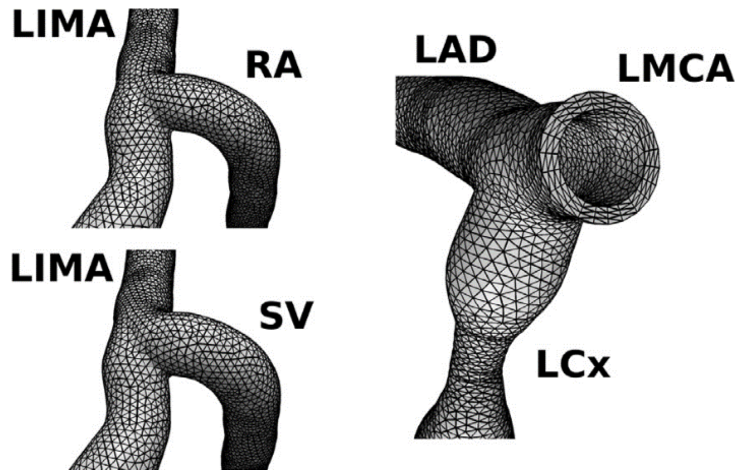

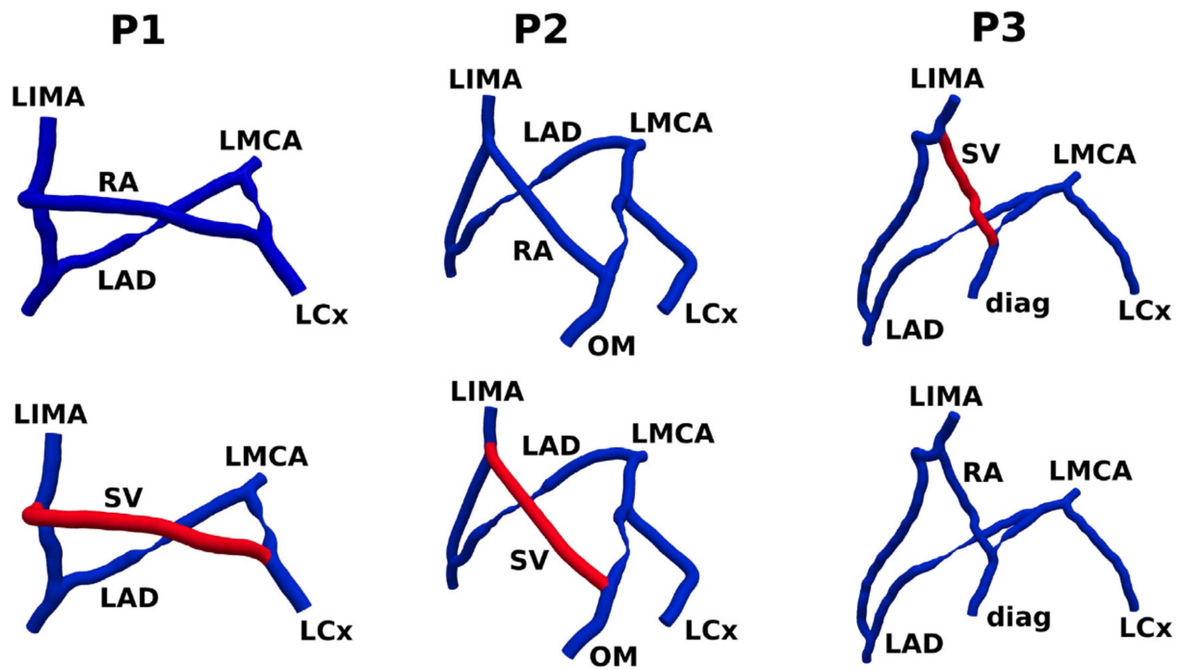

The virtual scenario is performed by changing the geometry (lumen and vessel wall) and the elastic properties (10^5 Pa for RA, 10^6 Pa for SV)

Models:

Fluid: Incompressible Navier-Stokes equations

Vessel wall: Hooke law (linear elasticity)

Partitioned algorithm (Robin-Robin)

LIFEV – www.lifev.org

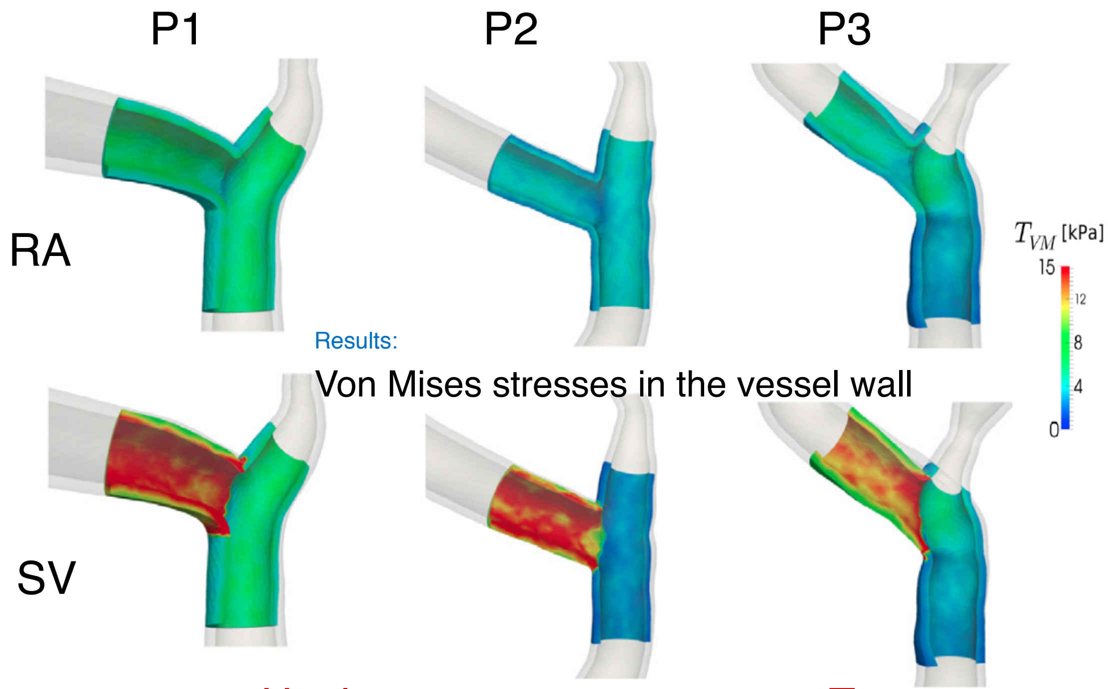

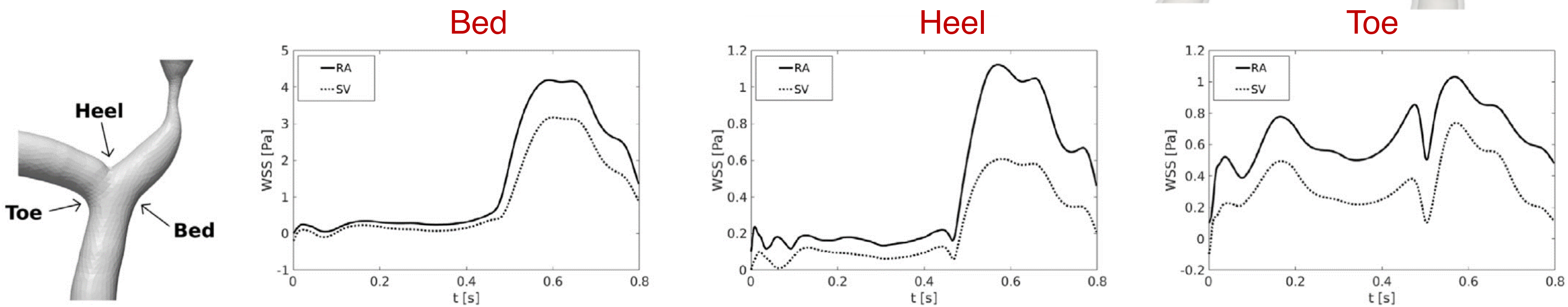

Radial artery by-pass seems to reduce conditions that could promote restenosis (high Von Mises stresess and low WSS)

Abdominal Aortic Aneurysm (AAA)

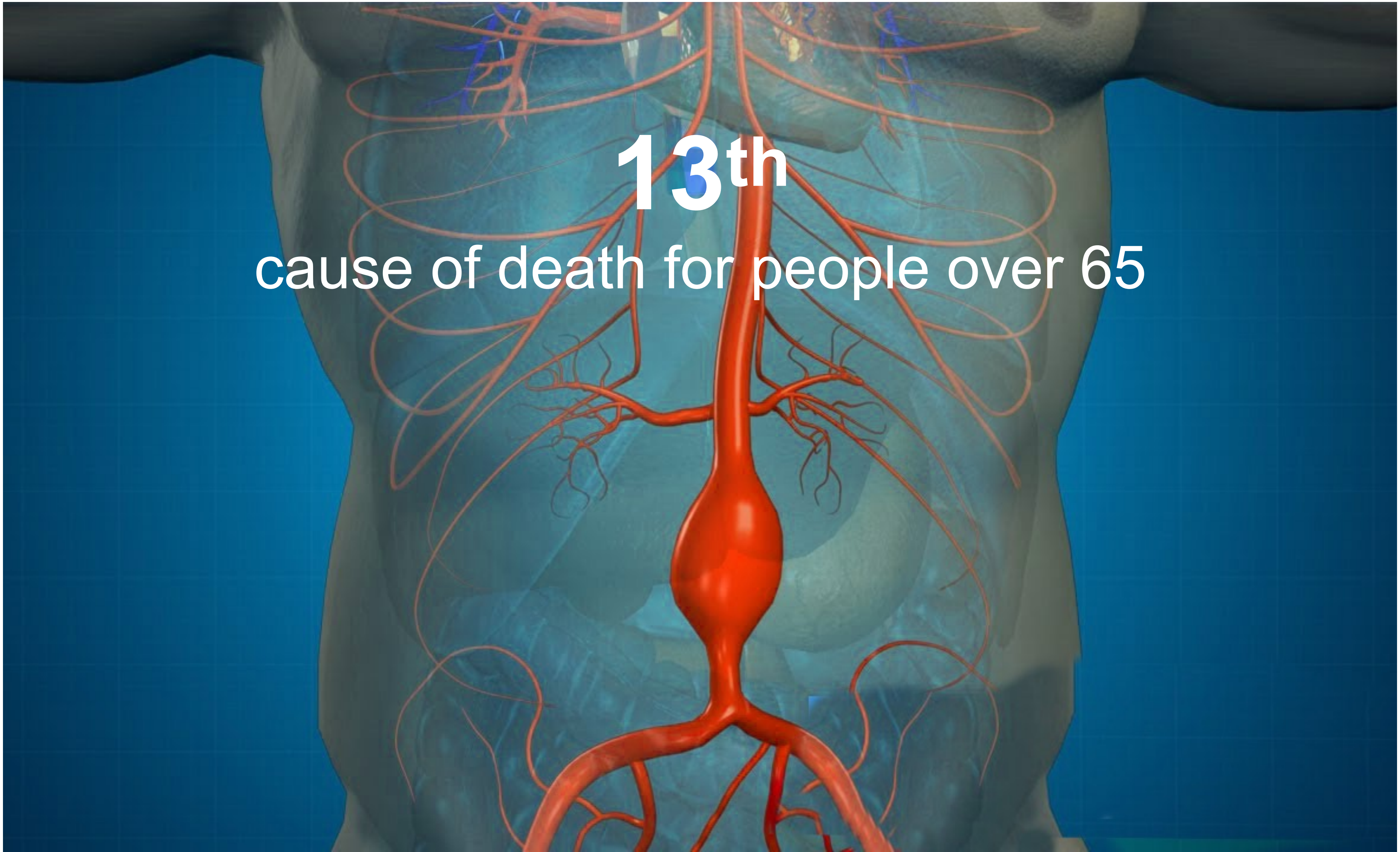

Numerical simulations for AAA

NUMERICAL MODEL SETUP - DISCRETIZATION

Finite Element Method

Fluid

P1-P1Bubble or P1-P2 FE

million equations

Structure

P2 Finite Elements

hundred thousand equations

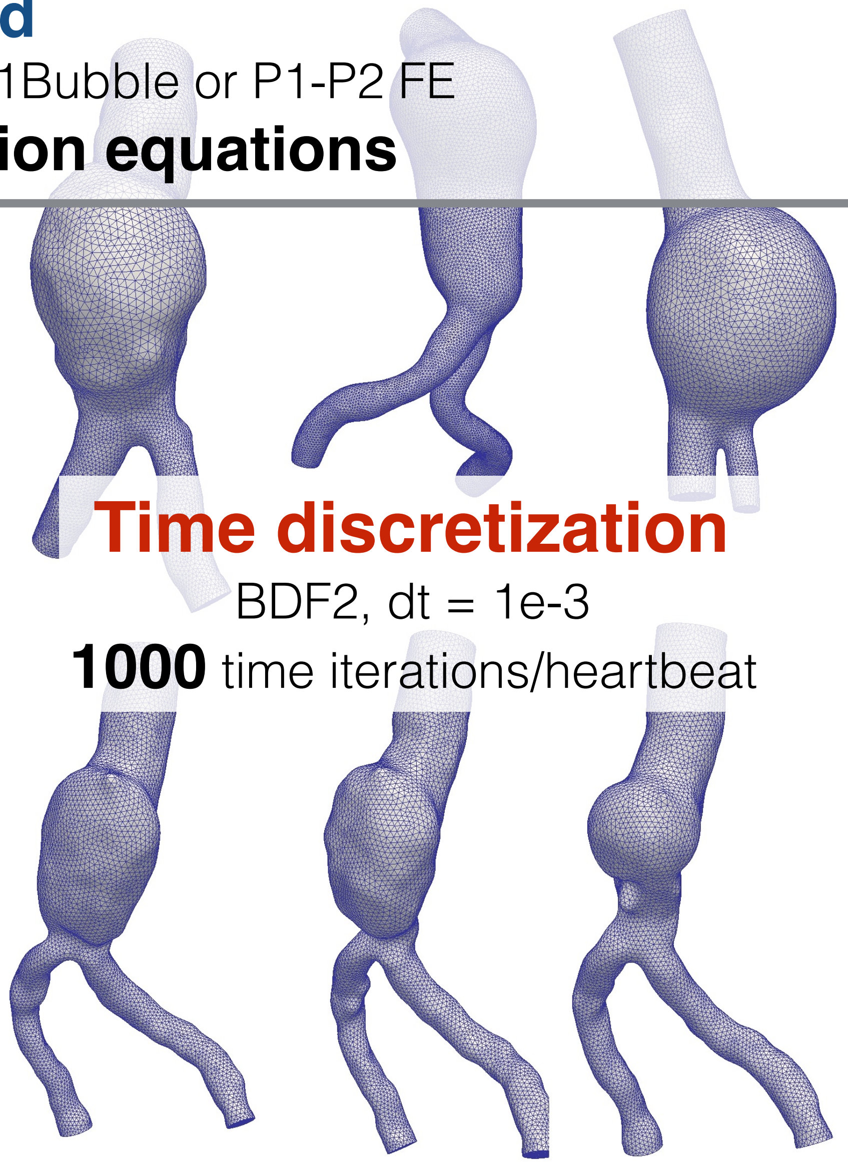

Time discretization

BDF2, dt = 1e-3

1000 time iterations/heartbeat

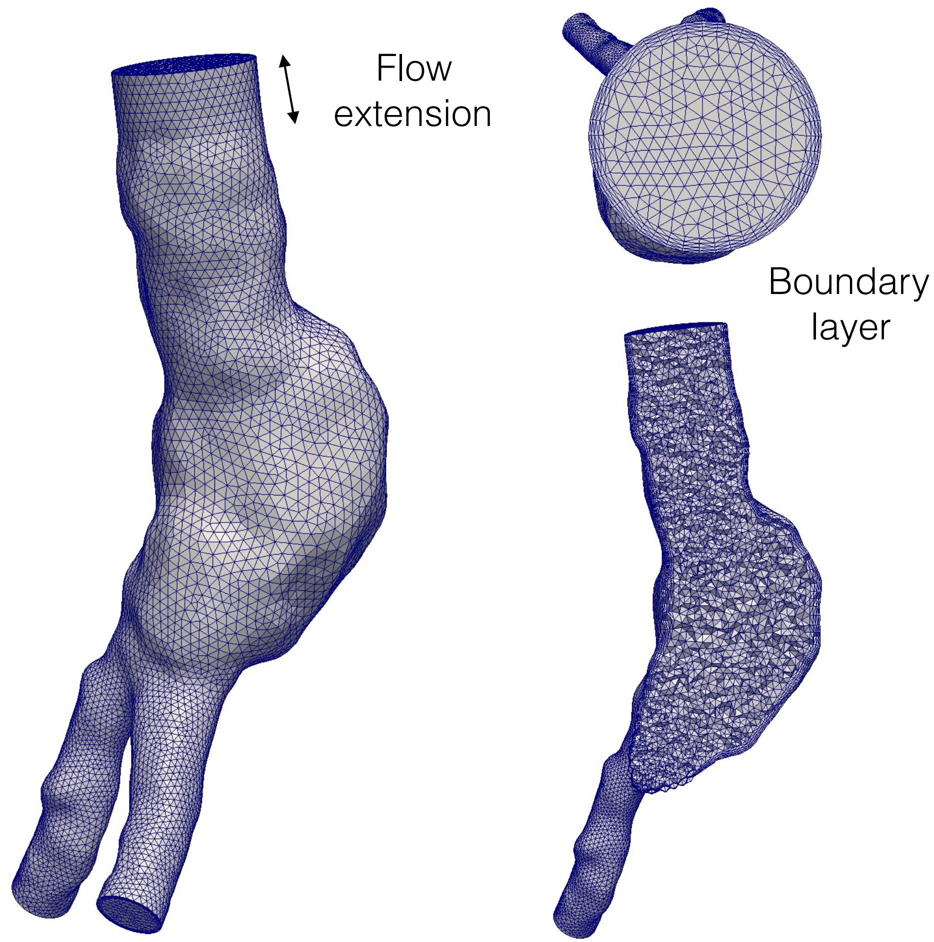

Numerical simulations for AAA

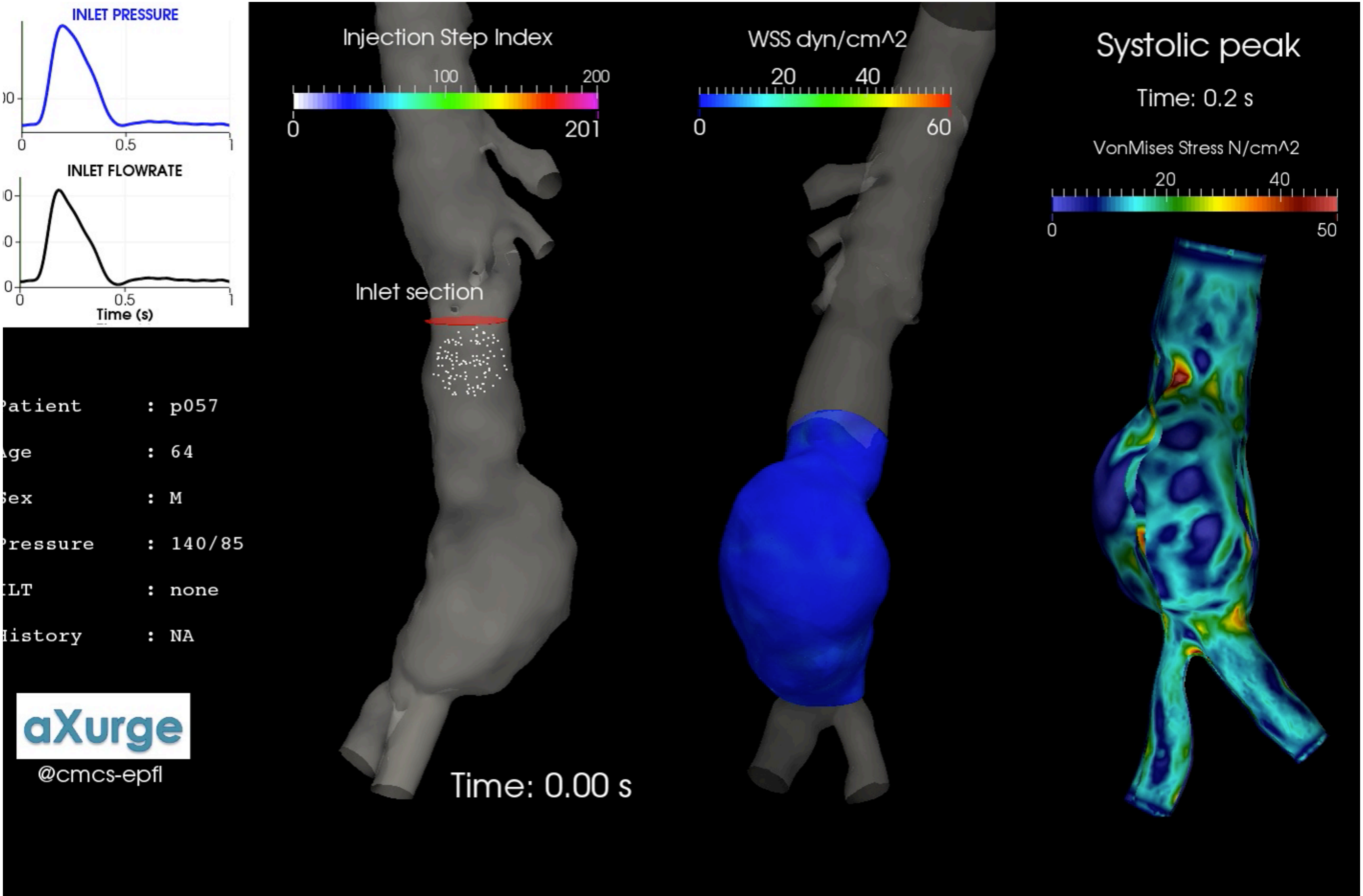

Platform Features

Imaging & Automatic Sizing

Accurate measurement of the aneurysm size

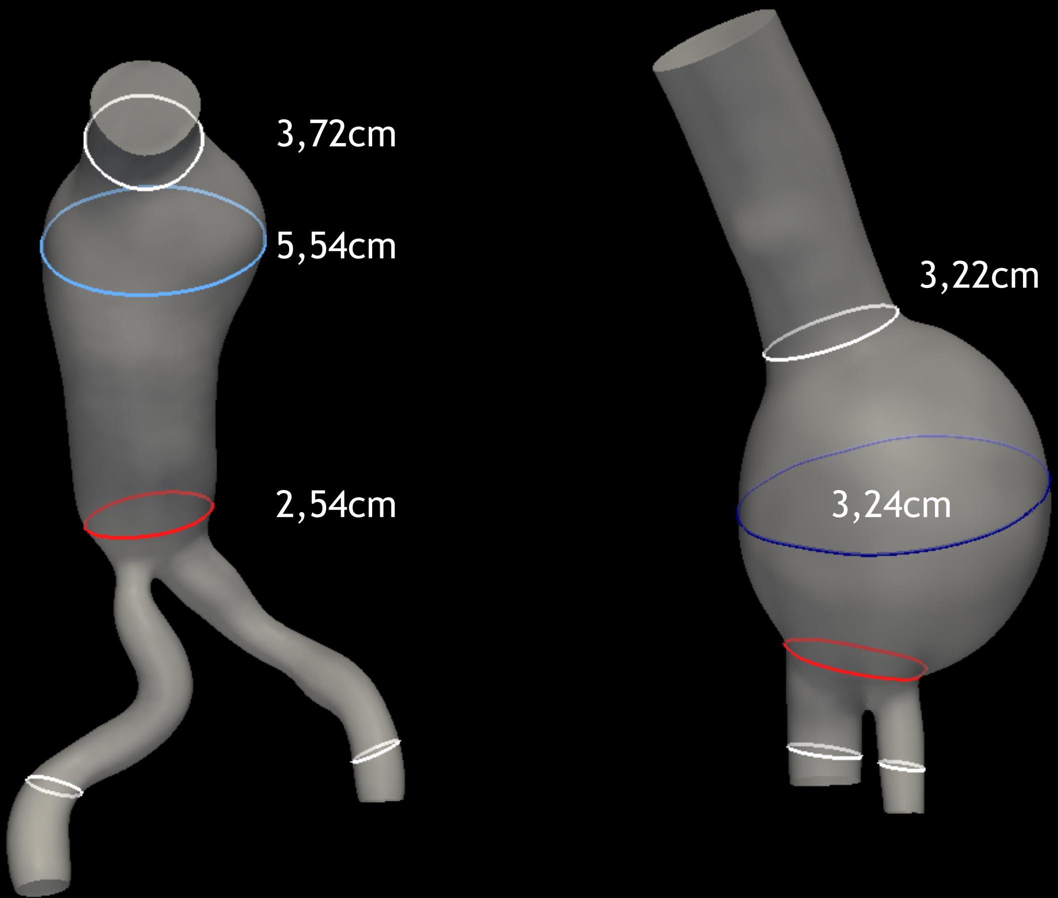

Platform Features

Advanced Numerical Simulation

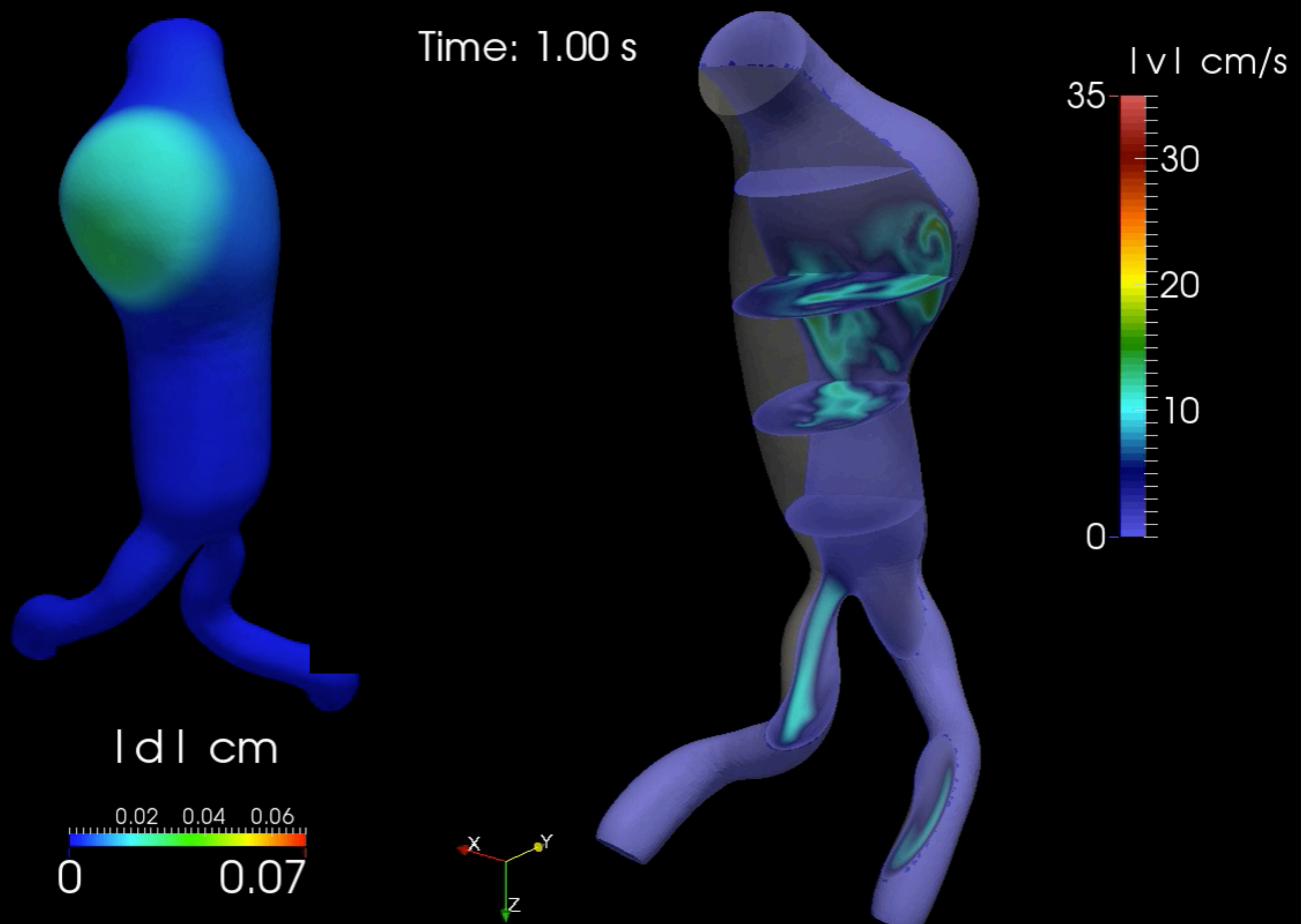

Platform Features

Maurizio Domanin
Vascular Surgeon
Università degli Studi di Milano

Smart Surgical Planner

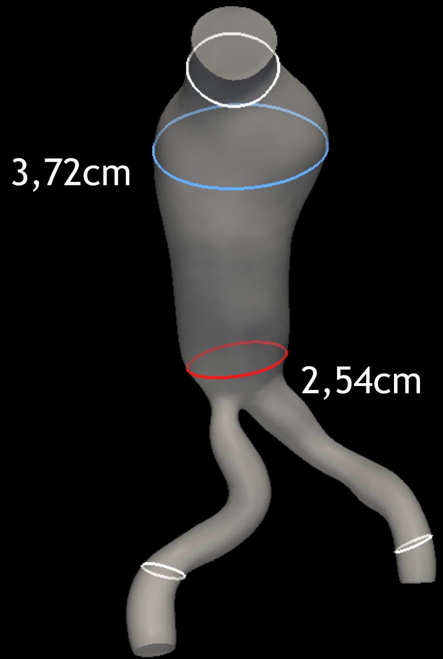

Automatic selection of the proper device